

## Observation of the periodicity of cloud rotation in Venus with Pirka telescope

Masataka Imai<sup>1\*</sup>, Yukihiro Takahashi<sup>1</sup>, Shigeto Watanabe<sup>1</sup>, Makoto Watanabe<sup>1</sup>, Ko Hamamoto<sup>1</sup>

<sup>1</sup>Department of CosmoSciences, Graduate School of Science, Hokkaido University

The Super-rotation, which is a phenomenon that Venusian atmosphere moves westward at a velocity 60 times faster than the solid planet rotation, is a unique atmospheric system of Venus. Its mechanism and even the fundamental properties, such as the variation of the rotation period, are still unknown. When we observe the Venusian atmosphere in ultraviolet range, the dark pattern, which is considered to represent the distribution of UV-absorber above the clouds, can be seen. The time variation of this pattern suggests the wind circulation of the atmosphere and/or the atmospheric wave propagating at an altitude of 70 km or higher, being related to the super-rotation. Del Genio & Rossow (1982, 1990) reported the brightness of the Venus cloud has a variation in periodicity changing from four to five days and this change occurred independently for each latitude band. Our purpose is to monitor this change of the period in brightness based on the long-term observation with Pirka telescope and to investigate its mechanism.

Multi-Spectral Imager (MSI) mounted on the 1.6 m Pirka telescope, owned and operated by the graduate school of science in Hokkaido University, is used to take UV images of Venus. The Pirka telescope is primarily dedicated to the observations of solar planets, and MSI can set the exposure time very short ( $\sim 0.04$  s) and change the center wavelength of narrow band transmittance using liquid crystal tunable filters rapidly. Thanks to Pirka telescope and MSI, we can observe in the daytime of the earth and monitor the planetary scale UV-features ( $> 5,000$  km) over 8 hours in 1 day with 1 or 2 month interval. Using MSI data, it is possible to investigate the time variation of cloud brightness in UV covering the full super-rotation time scale (over 4 days) and to compare the variations at different latitudes.

We estimated the brightness of each latitude band and calculated the relative brightness to equatorial region at 365 nm for the data observed in July 2012. Size of each examined area is  $10^\circ \times 10^\circ$  (longitude x latitude), which is larger than the atmospheric seeing size at the observation site. This method makes it possible to work through the problem of correcting the earth's atmosphere effect so that we can compare the time variations between different latitudes. We found the typical time variation seems to be related to the super-rotation. This results show piecewise continuous distribution of UV features in the direction of longitude and suggest that features propagate in synchronization among  $50^\circ\text{S} - 50^\circ\text{N}$ . For further investigation, we also analyze the VCM/Venus Express data to estimate the absolute change of brightness along some latitude band. We will be able to obtain the absolute brightness distribution for each latitude band from combining the MSI and the VMC data and to compare the results among different observation periods.

Keywords: venus, super-rotation, ground based observation, pirka telescope

## Estimation of wind at the cloud top of Venus

Shinichi Ikegawa<sup>1\*</sup>, Takeshi Horinouchi<sup>2</sup>

<sup>1</sup>Graduate School of Environmental Science, Hokkaido University, <sup>2</sup>Faculty of Environmental Earth Science, Hokkaido University

In this study, we used the UV images from the Venus Monitoring Camera (VMC) onboard ESA's Venus Express. We improved the cross-correlation method by using multiple images. This is because noise is reduced, and the effective degrees of freedom is increased.

Keywords: Venus, super-rotation, estimation of wind

## Numerical modeling of cloud-level convection on Venus

Takehito Higuchi<sup>1\*</sup>, IMAMURA, Takeshi<sup>2</sup>, MAEJIMA, Yasumitsu<sup>3</sup>, IKEDA, Kohei<sup>4</sup>, TAKAGI, Masahiro<sup>5</sup>, SUGIMOTO, Norihiko<sup>6</sup>

<sup>1</sup>The University of Tokyo, <sup>2</sup>Japan Aerospace Exploration Agency, <sup>3</sup>Meteorological Research Institute, <sup>4</sup>Japan Agency for Marine-Earth Science and Technology, <sup>5</sup>Kyoto Sangyo University, <sup>6</sup>Keio University

Venus is covered by clouds of sulfuric acid which float in the altitude region from 48 to 70 km. The clouds reflect about 80% of the incident sunlight and play a major role in the energy balance of Venus. A neutral stability layer has been known to exist at around 50-55 km in the middle and lower cloud region; this layer is considered as a region of convection driven by the heating of the cloud base by the upward thermal radiation from the lower atmosphere (Crisp et al., 1990). The convection is thought to play important roles in the transport of cloud-related materials, and thus constitutes an essential part of the cloud system.

On Venus, in a manner analogous to the Earth, energy fluxes of incoming shortwave radiation and outgoing longwave radiation do not balance each other out at each latitude: low latitudes are subjected to excessive shortwave heating, while high latitudes are subjected to excessive longwave cooling. Such energy imbalance should affect the structure of the cloud-level convection. Excessive heating and cooling occur also periodically with the period of the atmospheric super-rotation, because irradiation to a certain cloud-level air changes as it is advected by the super-rotation. Therefore, it is necessary to understand the latitude dependence and the diurnal variation of the structure of cloud-level convection. Baker et al. (1998; 2000) performed numerical experiments of cloud-level convection and studied the characteristics of convection such as the intensity, the aspect ratio and the penetration of plumes to the stable layer located above and below the convective layer. However, the latitude dependence and the diurnal variation were not addressed in their studies, and furthermore, their numerical model drives convection by diffusive heat fluxes from below and realistic radiative heating and cooling distributions were not introduced into the model.

In this study, I constructed a numerical model of cloud-level convection based on the non-hydrostatic meteorological model CReSS (Tsuboki and Sakakibara, 2007) and studied the latitude dependence and the diurnal variation of cloud-level convection. Longwave heating and cooling are taken from a one-dimensional radiative-convective equilibrium calculation for a globally-averaged condition made by Ikeda (2010), and shortwave heating is given as a function of the local time and the latitude. The magnitude of the vertical velocity is consistent with the Vega balloon measurements and the estimate by the mixing length theory, suggesting that the model reproduces convection of realistic strength. With respect to the latitude dependence, stronger and deeper convection occurs at high latitudes than at low latitudes. This result might explain the latitudinal tendency revealed by radio occultation observations that neutral stability layer in the cloud tends to be thicker (Tellmann et al., 2009) and gravity wave amplitudes are larger in the high latitude than in the low latitude (Tellmann et al., 2012). With respect to the diurnal variation caused by the advection of cloud-level atmosphere by the super-rotation, strong, deep convection occurs during nighttime rather than daytime. Such dependences on the latitude and the local time come from the unique mechanism of cloud-level convection: shortwave heating of the upper cloud layer suppresses convection, whereas longwave heating of the lower cloud and the longwave cooling of the upper cloud, which drive the cloud-level convection, do not vary much with the local time and the latitude.

Keywords: Venus, cloud, convection

## Origins of Contrasts in Venus Seen at Thermal Infrared and Near-Infrared Wavelengths

Takao M. Sato<sup>1\*</sup>, Hideo Sagawa<sup>2</sup>, Toru Kouyama<sup>3</sup>, Takeshi Imamura<sup>1</sup>, Takehiko Satoh<sup>1</sup>

<sup>1</sup>Institute of Space and Astronautical Science, Japan Aerospace Exploration Agency, <sup>2</sup>National Institute of Information and Communications Technology, <sup>3</sup>National Institute of Advanced Industrial Science and Technology

The middle atmosphere (60-100 km) of Venus plays an important role in determining its own environment. Venus is completely shrouded by a curtain of dense clouds (50-70 km) with total optical thickness of 20-40 at visible wavelengths. The upper sulfuric acid (H<sub>2</sub>SO<sub>4</sub>) clouds reflect ~76% of the incident solar radiation back to space. More than 70% of the solar energy absorbed by Venus is deposited at altitudes higher than 64 km mainly due to absorption of unknown UV absorbers mixed in the upper cloud. This horizontally and vertically unusual heating in the cloud layer excites the thermal tides, which are key process to understand the atmospheric super-rotation. In order to elucidate this mysterious atmospheric phenomenon, it is fundamental to investigate horizontal and vertical thermal structure in the middle atmosphere.

Mitsuyama et al. observed Venus at three thermal infrared (hereafter TIR) wavelengths (8.59, 11.24, and 12.81 micron) with the Cooled Mid-Infrared Camera and Spectrometer (COMICS), mounted on the 8.2-m Subaru Telescope, during the period of October 25-29, 2007. Thermal radiations at these wavelengths are most sensitive to altitudes of ~70 km. The spatial resolution of images was ~500 (km/pixel). This was the first time that such high spatial resolution full-disk images had been obtained. After processing images with high-pass filter, they found a horizontal Y-shape structure, which was similar to that seen in UV, varying its shape from day to day.

In this study, to understand what determine the observed contrast (1-2 K) of thermal radiations in equatorial latitudes at these TIR wavelengths, we investigate sensitivity of atmospheric parameters with radiative transfer calculations. A cloud model (Eymet et al., 2009) which is based on the results of Venera 15 (Zasova et al., 2007) is adopted in our calculations. There are four candidates that can be responsible for this contrast: temperature profile, cloud top altitude, and optical thicknesses of mode 1 and mode 2 particles. Conversely, optical thicknesses of mode 2' and mode 3 particles are not sensitive to thermal radiations at these TIR wavelengths. To narrow down the contrast source, we also examine the contrast of reflectance at 968 nm (hereafter NIR) obtained by Galileo Solid State Imager (SSI). From the calculation, the optical thicknesses of all the considered four cloud particles (mode 1, mode 2, mode 2', and mode 3) can reproduce the observed contrast of reflectance (1-2%) while the other parameters (temperature and cloud top altitude) are insensitive to reflectance. We find that variations of optical thicknesses of mode 1 and mode 2 particles can satisfy the observed contrasts both of TIR and of NIR simultaneously. However, it has been pointed out that the altitudes that contribute most to the observed radiance at NIR (58-64 km) are lower than those at UV (62-70 km) based on the results of cloud-tracked zonal velocity [e.g., Sanchez-Lavega et al., 2008]. It would suggest that optical thicknesses of mode 1 and mode 2 particles are less variable in equatorial latitudes and the obtained thermal contrasts seen in TIR result from the variation of temperature profiles and/or cloud top altitudes rather than those of optical thicknesses of mode 1 and mode 2 particles.

Keywords: Venus, Thermal infrared, Near-infrared

## Quantification of oxygen isotope ratios in the Venus atmosphere by IR spectroscopy

Naomoto Iwagami<sup>1\*</sup>, George HASHIMOTO<sup>2</sup>

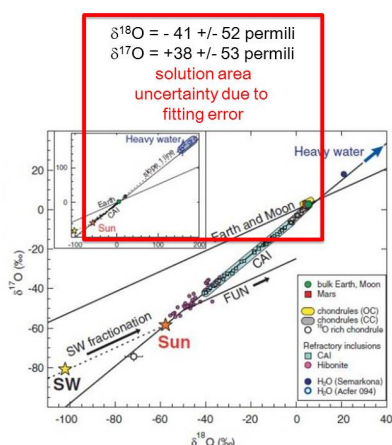
<sup>1</sup>University of Tokyo, <sup>2</sup>Okayama University

The oxygen isotope ratios  $^{17}\text{O}/^{16}\text{O}$  and  $^{18}\text{O}/^{16}\text{O}$  in the solar system are known to show a clear systematic relation. And the relation differs planet by planet. For example, the  $^{17}\text{O}/^{16}\text{O}$  ratio as a function of  $^{18}\text{O}/^{16}\text{O}$  ratio in Mars appears to be larger than that in the Earth-Moon system by 0.05 ‰. This fact indicates that the proto-Earth-Mars matter was so well mixed but with a systematic difference. In such a way, the isotope ratios may provide information about the origin and evolution of the planets. However,  $^{17}\text{O}/^{16}\text{O}$  ratio in Venus has never been quantified, and may provide further information about the mixing history of the early solar system if measured.

The ratios may be quantified by ground-based  $\text{CO}_2$  IR spectroscopic measurements. By assuming a use of IRTF CSHELL spectrometer with a nominal resolution of 40000, we looked for suitable wavenumber regions to quantify the  $^{17}\text{O}/^{18}\text{O}$  and  $^{18}\text{O}/^{16}\text{O}$  ratios. The suitable region for the former is found at  $2648\text{ cm}^{-1}$  as shown in the figure, and the latter at  $4582\text{ cm}^{-1}$ . In the figure, the top two curves show the earth and solar structures disturbing the quantification, and the middle two curves show the Venus  $\text{C}^{17}\text{O}^{16}\text{O}$  and  $\text{C}^{18}\text{O}^{16}\text{O}$  structures indicating a feasibility to quantify the  $^{17}\text{O}/^{18}\text{O}$  ratio.

isotope  
quest 3  
preliminary result

Error in HITRAN  
 $\Delta S \sim 2\text{-}5\%$  for  $^{17}\text{O}$   
 $\Delta S \sim 10\text{-}20\%$  for  $^{18}\text{O}$   
 $\Delta S \sim 10\text{-}20\%$  for  $^{16}\text{O}$



## Venus upper atmosphere derived from the Hinode's high resolution images acquired during the transit of Venus

Miho Kanao<sup>1\*</sup>, Masato Nakamura<sup>1</sup>, Toshifumi Shimizu<sup>1</sup>, Takeshi Imamura<sup>1</sup>, Alphonse Sterling<sup>2</sup>, Takeshi Sakanoi<sup>3</sup>, Yasumasa Kasaba<sup>3</sup>, Atsushi Yamazaki<sup>1</sup>

<sup>1</sup>ISAS, <sup>2</sup>NASA Marshall Space Flight Center, <sup>3</sup>Tohoku University

The solar satellite 'Hinode' observed the Venus transit of 5th and 6th Jun. 2012. Hinode's Solar optical telescope (SOT) detected a ring-shaped emission from the Venusian atmosphere between 1st contact (22:15:46) and 2nd contact (22:29:53). We studied data when the emission ranged from latitude N87 to S17 of Venus.

The estimated altitude of the ring emission ranges from 65km to 74km, where the altitude is lower in the northern polar region than in the mid-latitude region. The strength of the integrated emission along the altitude increases with higher latitude.

The emission is assumed to be the refracted solar light, and the refraction angle is calculated using a Venusian CO<sub>2</sub> atmosphere model with temperature and density parameters. We show that the refracted ray passes through Venus atmosphere from 50km to 90km altitude. Based on comparisons between the observations and calculations of the extinction coefficient of the Rayleigh scattering in the CO<sub>2</sub> atmosphere, we consider the distribution of the cloud particles in the Venus atmosphere.

Keywords: Venus upper atmosphere, Hinode

## Study of planetary atmospheric dynamics, photochemistry, and meteorology using Mid-Infrared LAsER Heterodyne Instrument

Hiromu Nakagawa<sup>1\*</sup>, Shohei Aoki<sup>1</sup>, Yasumasa Kasaba<sup>1</sup>, Isao Murata<sup>1</sup>, Shoichi Okano<sup>2</sup>

<sup>1</sup>Geophysics, Tohoku University, <sup>2</sup>University of Hawaii

In this paper, an overview of the science addressable with Mid-Infrared LAsER Heterodyne Instrument (MILAHl) will be given. The list is certainly not exhaustive and proposals for future projects are very welcome. With the configuration described below the instrument MILAHl can be used for research in the atmospheres of solar system objects, i.e. planets, moons, comets, the Earth and the Sun. Extra solar objects like stars and stellar envelopes, proto-planetary disks or even exoplanets are possible targets of interest. MILAHl is easily transportable and widely usable for second-generation instrument for the airborne observatory, and large telescope project at Antarctic (Ichikawa, private communications).

Many molecules of atmospheric and astronomical interest exhibit rotational-vibrational spectra in the middle infrared regime. Fully resolved molecular features with high spectral resolution are possible retrieval of many physical parameters, such as density, velocity, pressure, excitation condition, temperature, and the vertical information from single line profile.

In mid-infrared wavelength region, the highest spectral resolution is provided by the infrared heterodyne technique (Kostuik and Mumma, 1983). It is for the applications to astronomy and planetary atmospheric science in 7-13 micron wavelength at a spectral resolution of up to  $10^7$ -8 with a very high sensitivity. Infrared heterodyne spectroscopy has been applied to study of planetary atmosphere (Goldstein et al., 1991; Kostuik, 1996; Kostuik et al., 2000; Fast et al., 2006; Fast et al., 2011; Sonnabend et al., 2012; Sornig et al., 2012) to date.

We have developed a new infrared heterodyne instrument, called Mid-Infrared LAsER Heterodyne Instrument (MILAHl), for our dedicated new telescope (1.8m) at the summit of Mt. Haleakala, Hawaii. This project would be milestone in order to increase our understanding of various temporal variability (diurnal, seasonal, and solar cycle effect) of planetary atmospheric dynamics, photochemistry, and meteorology.

Remarkable advantages of this instrument are as follows: (i) ultra-high velocity resolution (up to 10 m/s, corresponding to  $10^7$  wavelength resolving power) with a bandwidth of two times 1 GHz, (ii) previously unheard of compactness within 1 plate (600mm x 600mm) including the calibrators, (iii) excellent system noise temperature less than 2700 K at 9.6 micron wavelength. In order to provide wider wavelength range, a room-temperature type quantum cascade laser was applied for the first time. Its operating spectral range achieved to be 5 cm<sup>-1</sup>. As the backend spectrometer, a compact digital FFT spectrometer was also first applied for our system in order to obtain (a) a high frequency resolution, (b) stability and flexibility, and (c) a wide dynamic range. In this paper, an expected S/N will be discussed using measured spectra of stratospheric ozone in the terrestrial atmosphere.

First light of this instrument would be performed in the summer 2013 at the same summit using our 60cm-telescope in the verification process. First candidates for test measurements are Mars and Venus.

**Keywords:** planetary atmosphere, infrared, heterodyne, spectroscopy, observation



## Monitoring Observations of the Middle Atmospheres of Solar Planets at Millimeter-Wave Band with SPART Telescope

Hiroyuki Maezawa<sup>1\*</sup>, Nayuta Moribe<sup>2</sup>, Hideo Sagawa<sup>3</sup>, Atsushi Nishimura<sup>1</sup>, Yoshinori Ikeda<sup>1</sup>, Shigeki Osaki<sup>1</sup>, Kouske Horiuchi<sup>1</sup>, Toshikazu Ohnishi<sup>1</sup>, Munetoshi Tokumaru<sup>2</sup>, Yasuo Fukui<sup>2</sup>, Akira Mizuno<sup>2</sup>, Shusaku Kondo<sup>2</sup>, Kazuyuki Handa<sup>4</sup>, Jun Maekawa<sup>4</sup>, Shigeru Takahashi<sup>4</sup>, Ryohei Kawabe<sup>4</sup>, Nario Kuno<sup>4</sup>

<sup>1</sup>Osaka Prefecture University, <sup>2</sup>Nagoya University, <sup>3</sup>National Institute of Information and Communications Technology, <sup>4</sup>National Astronomical Observatory

Investigation of the abundance and time variation of minor constituents of planetary atmospheres and of the isotopes of these constituents provides important information about the dynamical and chemical balances and evolutionary processes of the atmospheres. To study how activities of the Sun, a typical G-type star in our galaxy, influence the physical conditions and (photo)chemical reaction network of the middle atmospheres of Venus, Mars, and gas-giant planets, we started monitoring observations of the spectral lines of the minor constituents such as carbon monoxide ( $J = 1-0$ : 115 GHz) in the Martian and Venusian middle atmosphere by using the SPART (Solar Planetary Atmosphere Research Telescope) which is the 10-m single dish telescope taken from the Nobeyama Millimeter Array System of Nobeyama Radio Observatory of Japan. In 2012 we installed a 200 GHz band SIS heterodyne detector onto the SPART newly to apply the retrieval analysis to the spectral line data precisely. Updates of the instruments and the computer system with Linux/Python-software enabled us to carry out highly-efficient monitoring and on-the-fly mapping observations toward Venus and Jupiter as well as dark clouds at the 200 GHz Band remotely. We will present the current status of this project at the conference.

Keywords: Solar Planets, Planetary Atmosphere, Radio Telescope, Heterodyne Spectroscopy, Solar Activity



## Characteristics of the Martian magnetic flux ropes observed by the Mars Global Surveyor

Takuya Hara<sup>1\*</sup>, Kanako Seki<sup>1</sup>, Hiroshi Hasegawa<sup>2</sup>, David A. Brain<sup>3</sup>, Miho Saito (Hasegawa)<sup>1</sup>

<sup>1</sup>Solar-Terrestrial Environment Laboratory (STEL), Nagoya University, <sup>2</sup>ISAS/JAXA, <sup>3</sup>LASP, Univ. of Colorado at Boulder

Mars is a unique planet because it locally possesses strong crustal magnetic fields mainly located in the southern hemisphere [e.g., Acuna *et al.*, 1999]. The Martian electromagnetic environment can thus become highly complicated and variable, since the interplanetary magnetic field (IMF) embedded in the solar wind interacts with the Martian crustal magnetic fields. Whereas it is known that the Martian upper atmosphere is escaping to the interplanetary space due to the interaction with the solar wind [e.g., Lundin *et al.*, 1989; Barabash *et al.*, 2007], the contribution of crustal magnetic fields to atmospheric escape from Mars has not yet been well understood.

Flux ropes are characteristic magnetic field structures seen throughout the solar system, e.g., at the Sun, in the interplanetary space, and at the Earth magnetosphere often in association with substorms. Flux ropes are also observed at planets such as at Venus and Mars [e.g., Russell and Elphic, 1979; Vignes *et al.*, 2004], which do not possess a global magnetic field. Recently, Brain *et al.* [2010] found a large-scale isolated magnetic flux rope filled with Martian atmospheric plasma located downstream from the crustal magnetic fields with respect to the solar wind flow based on their analyses of the magnetic field and suprathermal electron measurements from the Mars Global Surveyor (MGS) spacecraft. They suggested that the magnetic flux rope could intermittently carry significant amounts of atmosphere away from Mars by a bulk removal process such as magnetic reconnection between the IMF and the crustal magnetic fields. They proposed that this process might occur frequently and account for as much as 10 % of the total present-day ion escape from Mars.

We here investigate characteristics of the Martian magnetic flux ropes based on a reconstruction method using the MGS magnetic field data. This method is referred as the Grad-Shafranov (GS) reconstruction technique, which is capable of recovering the two-dimensional spatial configuration of the magnetic flux ropes from single spacecraft data. We assumed that it has a magnetohydrostatic, two-dimensional magnetic field structure [Hu and Sonnerup, 2002]. Since there is no ion detector onboard MGS, we assumed a typical density and temperature of the Martian ionosphere at the spacecraft altitude in order to calculate the input thermal pressure for the model. It is also assumed that the spacecraft velocity is the dominant component causing apparent movement of the magnetic flux rope relative to the MGS spacecraft. The resultant structure can provide a reliable observational restriction on the spatial scales of magnetic flux ropes. We applied the GS reconstruction technique to approximately 80 magnetic flux rope events observed by MGS. In the presentation, we will report not only the dependences of the flux rope orientation on the solar zenith angle and the crustal magnetic field, but also the relationship between the magnetic flux rope axis derived from the GS method and the typical plasma convection direction. We will also discuss the characteristics of the size of the magnetic flux rope depending on the observed geographic location.

### References:

- Acuna *et al.* (1999), *Science*.
- Barabash *et al.* (2007), *Science*.
- Brain *et al.* (2010), *Geophys. Res. Lett.*
- Lundin *et al.* (1989), *Nature*.
- Hu and Sonnerup (2002), *J. Geophys. Res.*
- Russell and Elphic (1979), *Nature*.
- Vignes *et al.* (2004), *Space Sci. Rev.*

Keywords: Mars, Magnetic flux rope, Grad-Shafranov equation, Crustal magnetic field, Mars Global Surveyor, Non-magnetized planet

## Asymmetric penetration of solar wind perturbations down to 400-km altitudes at Mars observed by Mars Global Surveyor

Kazunari Matsunaga<sup>1\*</sup>, Kanako Seki<sup>1</sup>, Takuya Hara<sup>1</sup>, BRAIN, David A.<sup>2</sup>

<sup>1</sup>Solar-Terrestrial Environment Laboratory, Nagoya University, <sup>2</sup>Laboratory for Atmospheric and Space Physics (LASP), Univ. of Colorado at Boulder, USA

Since Mars has no intrinsic global magnetic field, the solar wind can directly interact with the Martian upper atmosphere. It is thought that solar wind encountering Mars can penetrate into the point where the solar wind dynamic pressure and the plasma thermal pressure in the Martian ionosphere are almost balanced and the shocked solar wind flow is deflected around the boundary. However, the actual interaction can be complicated because of the plasma processes and the existence of crustal magnetic fields. It has been also pointed out that the crustal magnetic fields can locally push the boundary between the solar wind and the Martian magnetic pileup region (MPB ; magnetic pileup boundary) upward and cause the asymmetric structure of MPB. [e.g., Brain et al., 2003] The Kelvin-Helmholtz (K-H) instability at the Martian ionopause is one of important candidate processes to cause the modification of the asymmetric structure of the ionopause. In the plane perpendicular to the interplanetary magnetic field (IMF), the convection flow in the induced magnetosphere due to the draped field around the planet causes the asymmetry of the radial electric field direction, i.e., the hemispheres of the upward and downward convection electric fields. In the hemispheres of the upward solar wind convection electric fields, the wavy structures at the ionopause surface generated by the K-H instability tend to be enhanced. This enhancement may make the shocked solar wind (magnetosheath) plasma penetrate into lower altitudes than usual [e.g., Terada et al., 2002]. The Mars Global Surveyor (MGS) observations showed that MPB typically located at 800~1200km altitudes in dayside. However, this boundary location can change significantly depending on solar wind conditions. While previous studies indicate that the solar wind can penetrate into lower altitudes than usual when the solar wind pressure is high [Brain et al., 2005], the frequency of the solar wind penetration and its quantitative dependence on the solar wind conditions are not yet well understood. In this study, we focused on penetration of the magnetosheath, down to 400-km altitude at Mars. Using MGS data, we investigated the observational frequency and characteristics of the penetration events. We used data from the MGS mapping orbits from April 1999 to November 2006, while the spacecraft was in a nearly circular orbit at ~400 km altitudes. The mapping orbit is a polar orbit fixed in the local time at 2 am/pm, and the spacecraft orbital period is roughly two hours. When MGS passed through the magnetosheath-like region, fluctuations of the magnetic field and the high-energy electron flux were increased [e.g., Crider et al., 2005]. We first selected the time intervals when the power spectral density of the magnetic field fluctuation above 0.1Hz was higher than 1000 nT<sup>2</sup>/Hz, and the differential electron flux above 400eV was greater than 5\*10<sup>4</sup>/(cm<sup>2</sup>\*s\*sr\*eV). Then, we eliminated inappropriate events such as the plasma sheet crossings by inspection. We identified 218 events for the period of interest. The dependence on the solar wind dynamic pressure around Mars, the polarity of IMF, and the motional electric field around Mars are investigated. We use both the solar wind proxy data by Brain et al. [2006] and the time-shifted ACE data. The results show that the penetration events tend to be observed during high solar wind dynamic pressure period. The ACE data indicated that, the occurrence frequency of the away polarity of IMF is almost comparable to that of the toward polarity. However, it was found that the penetration events tend to be observed during the away polarity of IMF in the northern hemisphere of Mars. This condition corresponds to the frequent observations in the upward electric field hemisphere and consistent with the asymmetric structure of MPB by the enhanced wavy structures at the ionopause generated by the finite Larmor radius effects in the K-H instability.

Keywords: Mars, Ionospheres, Solar wind, MGS, induced magnetic field, unmagnetized planet

## Modeling of the Martian atmosphere escape

Junji Miyazawa<sup>1\*</sup>

<sup>1</sup>Hokkaido University

Martian atmosphere is thin and dry. However, the evidences of water flows for several billion years ago are still on the surface of Mars. It suggests that the ancient Mars atmosphere was warm and moist. One of the reasons that the Mars atmosphere becomes thin is the outflow of the atmosphere to the space. Because of no intrinsic magnetic field, the solar wind affects strongly the Mars atmosphere/ionosphere. Although the various atmospheric outflow models are considered for the atmospheric escape, the details processes have not been clarified. We constructed a model of atmospheric escape including the effect of collisions, and obtained the distribution of the atmosphere around Mars. In this presentation, we will present the effect of the collision and the amount of atmospheric escape.

Keywords: Mars, Atmospheric Escaping

## A simulation study of the ancient Martian exosphere of Mars with a DSMC model

Kaori Terada<sup>1\*</sup>, Naoki Terada<sup>1</sup>

<sup>1</sup>Graduate School of Science, Tohoku University

In this paper, we investigate the ancient oxygen and hydrogen exosphere of Mars using a one-dimensional multi-species direct simulation Monte Carlo (DSMC) model. The evolution of thermal and non-thermal escape rates depends on the history of the solar EUV intensity. The astronomical observations of stars that are analogous to the sun shows the solar EUV luminosity is gradually decreasing. 3.7 billion years ago, from which the loss mechanisms that still active today are dominant, the solar EUV luminosity is estimated to have been about 7 times the present one. We estimate the exobase altitude and the temperature at the exobase level, and the rates of oxygen escape due to the dissociative recombination of  $O_2^+$  and atomic hydrogen Jeans escape for three different solar EUV intensity cases, which correspond to 1, 3, and 6 times the present low solar activity.

We use an upper thermosphere-exosphere full-particle model using a DSMC method coupled with a photochemical model. The DSMC method is a method of solving the Boltzmann equation and a common and effective approach for simulation of rarefied gas flow dynamics. Traditionally, a one-fluid approximation is used for modeling of thermosphere. But a one-fluid approximation is not sufficiently adequate at upper-thermosphere where the Knudsen number is larger than 0.01. In such a transition domain (between collision and collision less domains), the collision frequency is not high enough that the commonly used thermal conductivity coefficient is adequate and that physical quantities of each species are equal to each other.

The computed exobase temperature of H is lower than that of the other species (O, N<sub>2</sub>, CO<sub>2</sub>). A hydrostatic equilibrium of H is not established owing to thermal escape of H. It produces an upward flow and a thermal energy is converted to a flow energy. Even the exobase temperatures of O, N<sub>2</sub>, and CO<sub>2</sub> are significantly lower than those of previous studies. The differences are mainly caused by the difference in an approach of molecular thermal conductivity.

## Hydrodynamic escape from early terrestrial atmospheres and effects of solar flares

Naomichi Furuhashi<sup>1</sup>, Kaori Terada<sup>1</sup>, Takanori Sasaki<sup>2</sup>, Kanako Seki<sup>3</sup>, Hitoshi Fujiwara<sup>4</sup>, Naoki Terada<sup>1\*</sup>, Yasumasa Kasaba<sup>1</sup>

<sup>1</sup>Graduate School of Science, Tohoku University, <sup>2</sup>Graduate School of Science and Engineering, Tokyo Institute of Technology,

<sup>3</sup>Solar-Terrestrial Environment Laboratory, Nagoya University, <sup>4</sup>Faculty of Science and Technology, Seikei University

There are very small H<sub>2</sub>O contents in the atmosphere and on the surface of contemporary terrestrial planets compared to the H<sub>2</sub>O contents in proto-atmosphere and in accreting materials during the late-stage accretion. To remove this large H<sub>2</sub>O contents, massive escape to space and/or to underground is needed. Hydrodynamic escape is a mechanism that could cause a massive atmospheric escape and largely influence the evolution of planetary atmospheres. In this study, we investigated quantitatively the effects of hydrodynamic escape on the evolution of early terrestrial atmospheres, and also the effects of solar flares on the hydrodynamic escape process. Hydrodynamic escape is a sort of thermal escape of neutral gas, driven by a strong X-ray and extreme ultraviolet (EUV) radiation that causes expansion and upward flow of a planetary atmosphere. On the other hand, solar flare is accompanied by a rapid increase in X-ray and EUV radiation, leading to the temporal heating of the upper atmosphere of a planet. It is pointed out that solar flares in early days (solar age of 0.1 Gyr) were about two orders of magnitude stronger than the present-day solar flares and such huge flares occurred a few times a day (Audard et al., 1999). Therefore, it is important to study the influences of solar flares on the early terrestrial atmospheres. However, previous models have a difficulty in investigating the effects of solar flares. For example, the model of Tian et al. (2008) cannot trace time variation and that of Sasaki (2007) does not consider the effects of CO<sub>2</sub>-15 micrometer cooling and chemical reactions. So, in this study, we tried to develop a numerical transonic hydrodynamic escape model to trace the time variations, and as a first step, we investigated the escape rates and the structures of a hydrogen-rich atmosphere for Earth, Venus and Mars conditions, and also their responses to solar flares.

First, we investigated the escape rates and the structures of a hydrogen-rich atmosphere for solar ages of 4.56 Gyr, 1.0 Gyr and 0.1 Gyr for Earth, Venus and Mars. As a result, it is found that for the hydrodynamic escape, the planetary mass is more important than the intensity of X-ray and EUV radiation. The heavier planetary mass is, the more influenced by the increase in X-ray and EUV radiation. Also, it is found that the initial H<sub>2</sub>O inventories estimated by Raymond et al. (2006) could not be removed by the hydrodynamic escape for Earth but could be for Mars throughout their histories.

Second, we investigated the effects of solar flares on the hydrodynamic escape for the Earth's mass and orbit condition. Solar X-ray and EUV radiation is changed up to 60 times more intense for 1-20 nm wavelength range and up to 6 times for 20-105 nm. As a result, the exobase temperature of a hydrogen-rich atmosphere rises by about 12K in 1.5 hours and keeps about 6K higher than the pre-flare level for more than 8 hours after a solar flare. Then, it takes a week to recover to the pre-flare level. Also, the escape rate calculated at the exobase rises up to 4 times in 2 hours after a solar flare. The escape rate at the upper boundary (20 planet radii) rises up to 1.5 times. Both the escape rates at the upper boundary and the exobase keep about 10% higher than the pre-flare levels for a week. For a sequence of solar flares, we find the cumulative effect on the escape rate and the exobase temperature.

Keywords: Atmospheric escape, Atmospheric evolution, Venus, Mars, Earth

## Temporal variation of Mercury's sodium density by observed using ground-based telescope at Haleakala observatory

Ayaka Fusegawa<sup>1\*</sup>, Hayato Dairoku<sup>1</sup>, Shingo Kameda<sup>1</sup>, Masato Kagitani<sup>2</sup>, Shoichi Okano<sup>2</sup>

<sup>1</sup>Rikkyo Univ., <sup>2</sup>Tohoku Univ.

Mercury has a thin atmosphere. In the past, Mercury has been observed by Mariner 10 and MESSENGER, and ground-based observations have also been carried out. H, He, O, Na, Mg, K, and Ca were detected in its atmosphere. Solar-photon-stimulated desorption, sputtering by impacting solar particles, and meteoroid vaporization are considered to be the source processes of Mercury's exosphere. However, the primary process among these three processes is unknown as yet. The resonance scattering constitutes exospheric emission. The NaD emission is well suited for study by ground-based observations because of its high intensity. Past observations have shown that the temporal variation and north-south asymmetry of intensity of sodium emission.

We have observed Mercury's sodium exosphere at the Haleakala Observatory in Hawaii since April 2011. The observations were performed using a 40 cm Schmidt-Cassegrain telescope, a high-dispersion spectrograph, and a CCD camera. We determined the temporal variation of the sodium density using the observational data. It is possible that the temporal variation of the sodium density is caused by variation of solar wind magnetic field if solar wind ion sputtering is the primary source process of Mercury's exosphere. To verify this assumption, we checked the temporal variation of solar wind magnetic field observed by MESSENGER, and then we compared these variations with our observational result.

CMEs toward Mercury probably cause the increase of the sodium density. Potter et al. (1999) suggested that the total amount of sodium on Mercury increased monotonically during several days of observation after CMEs occurred on the same side of the Sun as Mercury. We observed Mercury's sodium exosphere on November 23, 2011 when MESSENGER observed variation of solar wind magnetic field, which indicated CMEs arrived at Mercury. Despite this, our results have not shown large variation of the sodium density like that of Potter et al. (1999). From these results, we discuss the source processes of Mercury's exosphere.

**Keywords:** Mercury's exosphere, sodium, ground-based observation



## Numerical Modeling of Moist Convection in Jupiter's Atmosphere: the mechanism of the intermittent cloud activity

Ko-ichiro SUGIYAMA<sup>1\*</sup>, Kensuke Nakajima<sup>2</sup>, Masatsugu Odaka<sup>3</sup>, Masaki Ishiwatari<sup>3</sup>, Kiyoshi Kuramoto<sup>3</sup>, Seiya Nishizawa<sup>4</sup>, Yoshiyuki O. Takahashi<sup>5</sup>, Yoshi-Yuki Hayashi<sup>5</sup>

<sup>1</sup>Institute of low temperature science, Hokkaido University, <sup>2</sup>Graduate school of Science, Kobe University, <sup>3</sup>Department of Cosmo-sciences, Graduate School of Science, Hokkaido University, <sup>4</sup>RIKEN AICS, <sup>5</sup>Graduate school of Science, Kobe University

The mean vertical profiles of temperature, condensed components, and condensible gases in the cloud layer of Jupiter's atmosphere is thought to be maintained by the statistical contribution of a large number of clouds driven by internal and radiative heating/cooling over multiple cloud life cycles. For the purpose of investigating the above problem, we developed a two-dimensional cloud resolving model that incorporates condensation of H<sub>2</sub>O and NH<sub>3</sub> and production reaction of NH<sub>4</sub>SH and investigated a possible cloud layer structure in Jupiter's atmosphere with using the model (Sugiyama et al., 2009, Nagare Multimedia; Sugiyama et al., 2011, GRL, 38, L13201). Prominent result obtained in Sugiyama et al. (2011) is intermittent emergence of vigorous cumulonimbus clouds rising from the H<sub>2</sub>O condensation level to the tropopause. Due to the active transport associated with these clouds, the mean vertical distributions of cloud particles and condensible gases are distinctly different from the hitherto accepted three-layered structure based on the thermodynamical equilibrium calculations. However, they did not perform enough discussion about a mechanism that causes their most remarkable characteristic, intermittent emergence of vigorous cumulonimbus clouds. In this presentation, we investigate the above character in detail and discuss the mechanism.

Saw-tooth like temporal variation of overall temperature synchronizing with the intermittent cloud activity obtained in our calculations means that the intermittent cloud activity is caused by the fact that amount of heating due to H<sub>2</sub>O condensation of the vigorous cumulonimbus clouds is quite large compared to the body cooling that is a substitute for radiative cooling. At the start of the active cloud development, downward plumes that reach below the H<sub>2</sub>O condensation level trigger the release of latent instability; vigorous cumulonimbus clouds develop due to returning updrafts associated with the downward plumes. At the end of the active cloud development, relatively heavy air parcel containing large amount of condensible gases cannot rise from H<sub>2</sub>O condensation level to the tropopause. The condition of the termination of the active periods can be quantitatively expressed as that the value of cloud work function (Arakawa and Schubert, 1974), which is a vertical integrated measure of buoyancy, is almost zero. The period of the intermittency is roughly estimated by using both the temperature variation due to the intermittency and the radiative cooling rate.

Keywords: Jupiter's atmosphere, moist convection, numerical modeling, cloud resolving model



## Multi-spectral imaging of jupiter's circumpolar wave

Ko Hamamoto<sup>1\*</sup>, Yukihiro Takahashi<sup>1</sup>, Makoto Watanabe<sup>1</sup>, Shigeto Watanabe<sup>1</sup>, Tetsuya Fukuhara<sup>1</sup>, Mitsuteru Sato<sup>1</sup>, Masataka Imai<sup>1</sup>, Akihito Ozaki<sup>1</sup>

<sup>1</sup>Department of CosmoSciences, Graduate School of Science, Hokkaido University

Jupiter's polar region is covered by haze, which is bright in images taken in the strong methane absorption band around 889 nm. The edge of polar haze region shows circumpolar wave with averaged zonal wavenumbers of 12 at planetographic latitude of -67 degrees. Previous studies showed that the zonal wave velocity has annual variability, however, variation in few months is uncertain because of poor sampling period of previous observations. Furthermore, the polar wave was only detected at 889 nm, there is no observation to detect the circumpolar wave at another wavelength in methane absorption band indicates different altitude.

In this study, to investigate the variation of zonal velocity of the circumpolar wave in time scale shorter than a year, we continually observed Jupiter in 5 terms from 2011 to 2012 using 1.6-m Pirka telescope and multi-spectral imager. In these observations, images were captured at wavelengths of 727 nm, 750 nm and 889 nm, corresponding to continuous, medium methane absorption and strong methane absorption, respectively. From data analysis of these observations, we recognized wave structures at 727 nm and 889 nm at -67 degrees. We conclude that the zonal wave velocity is smaller than ~3 m/s during the period from October to November in 2011, which is consistent to previous observations.

In addition to above observations, we conducted the spectral scan of Jupiter in strong methane absorption band (872 - 950 nm), at 3 nm step to investigate the vertical structure of the circumpolar wave. As a result, we succeeded in imaging the different feature of horizontal wave structure.

In future work we will try to detect the variation of the zonal wave velocity in a period shorter than a year. Furthermore, we will calculate the sounding level of each wavelengths in methane absorption band and estimate quantitatively the vertical variation of the wave structure.

Keywords: Jupiter, haze, circumpolar wave, ground-based observation

## The direct observation of the vertical profile of the Jovian H<sub>2</sub> and H<sub>3</sub><sup>+</sup> IR auroral emissions

Takeru Uno<sup>1</sup>, Takeshi Sakanoi<sup>1</sup>, Yasumasa Kasaba<sup>1\*</sup>, Masato Kagitani<sup>1</sup>, Chihiro Tao<sup>2</sup>, Sarah Badman<sup>3</sup>

<sup>1</sup>Dep. Geophysics, Tohoku Univ., <sup>2</sup>LPP, Ecole Polytechnique, <sup>3</sup>Univ. Leicester

Jupiter has the strongest and largest magneto-sphere in the solar system, energized by its strong magnetic field and fast planetary rotation. It is

driven by the dynamical and electromagnetic coupling between the Magnetosphere, Ionosphere, and Thermosphere.

This MIT coupling system is the key element for the energy transfer from planetary rotation to overall electro-magnetic activities like intense aurora.

The investigation of this strong system is important for comparative understanding of other magnetospheres, i.e., Earth, Sun, stars, high-energy objects, etc.

We have studied this system by numerical simulations (ex. Tao et al., 2009, 2010) and have compared them with infrared aurora (2-4 microns) taken with a ground-based telescope.

These emissions are from the Jovian polar atmosphere at sub-microbar pressure level (the Pedersen conducting layer), where is the key region for the MIT coupling.

Since the Jovian atmosphere mainly consists of hydrogen molecules, the dominant auroral emission lines are H<sub>3</sub><sup>+</sup> and H<sub>2</sub>.

The former represents the plasma component, produced by high-energy electrons injected from the magnetosphere through ion chemistry and excited by thermal collisions in the ionosphere.

The latter is from the neutral component, caused by the thermal excitation.

The evolution of the techniques of infrared observation enabled the detection of the infrared aurora of the outer planets from ground-based telescope.

In our CSHELL observation in Aug.-Sep. 2009, we got the maps of brightness of Jovian H<sub>3</sub><sup>+</sup> aurora at 4  $\mu$ m and H<sub>2</sub> aurora at 2.12  $\mu$ m.

It clearly shows morphological difference in the southern polar region.

In Sep.-Oct. 2010, we have observed Jovian H<sub>2</sub> and H<sub>3</sub><sup>+</sup> lines at 2.1  $\mu$ m in the auroral zone using SUBARU/IRCS.

The wide spectral coverage (1.96 - 2.42  $\mu$ m) and high spectral resolution ( $R = 20,000$ ) of SUBARU/IRCS, allowed us to derive the spatial distributions of neutral temperature.

But, no obvious difference of H<sub>2</sub> and H<sub>3</sub><sup>+</sup> morphologies was detected, due to the CML which is unsuitable for Northern aurora.

Keywords: Jupiter, infrared, aurora, H<sub>3</sub><sup>+</sup>, H<sub>2</sub>

## NIIHAMA Project: Continuous monitoring of Jupiter's infrared auroras

Takehiko Satoh<sup>1\*</sup>, Masaki Fujimoto<sup>1</sup>, Masato Kagitani<sup>2</sup>, Shoichi Okano<sup>3</sup>, Pierre Martin<sup>3</sup>, Jeff Kuhn<sup>3</sup>

<sup>1</sup>Japan Aerospace Exploration Agency, <sup>2</sup>Tohoku University, <sup>3</sup>University of Hawaii

The physics in the voluminous magnetosphere of Jupiter is made complicated by the strong magnetic field with fast rotation (~10 hours), and by significant amount of plasma that originates from a volcanic satellite, Io. Jupiter's auroras were known since 1970's but the mechanism of its production and maintenance still poorly understood to date. NIIHAMA project is thus motivated to perform long-term continuous monitoring of Jupiter's infrared auroras with a specifically-designed infrared camera attached to UHH's Hoku Kea Telescope.

NIIHAMA is an acronym of "Near-Infrared Imager on the Hoku keA telescope for Monitoring of Auroras". The camera was developed based on the technology that was used for the 2-um IR camera on board Japan's Venus Climate Orbiter, Akatsuki. The detector is a 1024x1024 PtSi array manufactured by Mitsubishi Electric, Co., Japan. Four filters (J, H, K, and 3.4-um for Jovian aurora) are installed in a 6-position filter wheel. The entire system has been developed by Sumitomo Heavy Industries, Ltd., Japan

(located in Niihama, Ehime).

As the Sun rotates with about a month of rotation period, the sector structure of the solar-wind plasma at vicinity of the Sun periodically changes. Our strategy with NIIHAMA is to monitor the auroras continuously for a month or a bit longer to effectively separate the intrinsic activity of Jupiter's magnetosphere from the solar-wind influence at Jupiter's orbit. This kind of study will be done within Jupiter's magnetosphere when the USA's JUNO spacecraft arrives at Jupiter in 2016. The ground-based study

with NIIHAMA will provide, from Hilo, Hawaii, useful and valuable precursor information before "in-situ" measurements are done with far more expensive spacecraft mission. Coordinated observation with the soon-to-be-launched SPRINT-A/EXCEED should also be very valuable.

## Investigation of the solar UV/EUV heating effect on the Jovian radiation belt based on radio/infrared observation

Hajime Kita<sup>1\*</sup>, Hiroaki Misawa<sup>1</sup>, Anil Bhardwaj<sup>2</sup>, Fuminori Tsuchiya<sup>1</sup>, Takeru Uno<sup>3</sup>, Chihiro Tao<sup>4</sup>, Takeshi Sakanoi<sup>1</sup>, Yasumasa Kasaba<sup>3</sup>, Akira Morioka<sup>1</sup>

<sup>1</sup>Planetary Plasma and Atmospheric Research Center, Tohoku University, <sup>2</sup>SPL, Vikram Sarabhai Space Centre, <sup>3</sup>Planetary Atmosphere Physics lab., Tohoku University, <sup>4</sup>Laboratoire de Physique des Plasmas, Ecole Polytechnique

In order to confirm the solar UV/EUV heating effect on the Jovian Synchrotron Radiation (JSR), we made coordinated observations using radio interferometer and infrared telescope. JSR is the emission from relativistic electrons in the Jovian radiation belt, and it is the most effective probe for the dynamics of the Jovian radiation belt through remote sensing from the Earth. It is theoretically expected that the solar UV/EUV heating for the Jovian thermosphere drives neutral wind perturbations, then the induced dynamo electric field increases radial diffusion. The solar UV/EUV heating is also expected to change the brightness distribution of JSR; i.e. the global enhancement of radial diffusion causes inward shift of equatorial emission peak position.

Previous studies confirm that the total flux density of JSR varied corresponding to the solar UV/EUV variations though it is unclear whether the temperature of the Jovian thermosphere actually varied during this event. The purpose of this study is to confirm whether sufficient solar UV/EUV heating occurs on the Jovian thermosphere and it actually causes the variations of the total flux density and brightness distribution. We made coordinated observations of the Giant Metrewave Radio Telescope (GMRT) and the NASA Infra-Red Telescope Facility (IRTF). From the radio interferometer, we measured the total flux density and brightness distribution of JSR. From the infrared spectroscopic observations, we estimated the temperature variations of the Jovian upper atmosphere from  $H_3^+$  emission.

The GMRT observations were made from 6th Nov to 17th Nov in 2011 at the frequency of 235/610MHz. The IRTF observations were made from 7th Nov to 12th Nov. We used high spectral resolution spectrometer, CSHELL, and observed  $H_3^+$  Q(1,0-) 3.953 microns emission. Slit position was located along the sub-solar point and dusk side limb. During the period, solar UV/EUV flux variations expected on Jupiter increased monotonically. The GMRT 610 MHz observation shows that the total flux density increased from 6th Nov to 13th Nov by about 5%, corresponding to the solar UV/EUV variations. The IRTF observation shows that equatorial  $H_3^+$  emission also increased from 7th Nov to 12th Nov by 20-30%, that is, temperature at the equatorial region was expected to increase. On the other hand, radio images showed that the equatorial emission peak position moved outward by 0.2 Jovian Radii.

These observation results showed that the variation of JSR at this time was caused by not global but non-uniform enhancement of radial diffusion. This non-uniform change can be explained by a numerical simulation study of the Jovian upper atmosphere. It is expected that temperature variations induced by the solar UV/EUV enhancement propagate from the auroral latitude to the low latitude region. These temperature variations cause enhancement of radial diffusion at the outer region which shift the equatorial peak position outward. Hence, we propose the scenario that radial diffusion increased not globally but locally at the outer region only around  $L=2-3$  during this period.

The further confirmation of the solar UV/EUV heating effect on the Jovian radiation belt is deferred to future studies in ground-based observations. Detail mapping of  $H_3^+$  emission and daily base observation is necessary to confirm that the temperature variations actually propagate from the auroral latitude to the low latitude region. In addition to that, temperature measurement using intensity ratio of  $H_3^+$  emission line is needed for more reliable results.

Keywords: Jupiter, Radiation Belt, Thermosphere, Radio Interferometer, Infrared

## Plasma density and temperature in Saturn's ionosphere

Shotaro Sakai<sup>1</sup>, Shigeto Watanabe<sup>1\*</sup>

<sup>1</sup>Department of Cosmo sciences, Hokkaido University

An average electron density in Saturn's mid-latitude ionosphere obtained from radio occultations by Cassini spacecraft was about  $10^4 \text{ cm}^{-3}$  at the altitude of 2000 km where density had a peak and gradually decreased with the increasing altitude. It was about  $100 \text{ cm}^{-3}$  at the altitude of 10000 km. The topside temperature is about 650 K. Plasma densities calculated by some models also were similar to the observations. However, electron densities from those models were calculated at the altitude below 4000 km. We have developed a plasma density-temperature model of Saturn's mid-latitude ionosphere including the magnetospheric effects. We used the magnetospheric plasma density and temperature as outer boundary conditions. The ion density is about  $10^4 \text{ cm}^{-3}$  at the altitude of 2000 km. It is similar to the densities from radio occultations. On the other hand, temperature is 2000 K or higher at the altitude of 2000 km. The higher temperature is necessary if the density is about  $100 \text{ cm}^{-3}$  at the altitude of 10000 km. In this presentation, we will also discuss how the magnetospheric ion is affected by ionospheric environments (e.g. ionospheric conductivity and temperature).

Keywords: Saturn, Ionosphere, Magnetosphere-ionosphere coupling

## Universal time control of AKR: Earth is a spin-modulated variable radio source

Akira Morioka<sup>1\*</sup>, Yoshizumi Miyoshi<sup>2</sup>, Satoshi Kurita<sup>1</sup>, Yasumasa Kasaba<sup>1</sup>, Hiroaki Misawa<sup>1</sup>, Hirotugu Kojima<sup>3</sup>

<sup>1</sup>Tohoku Univ., <sup>2</sup>STEL, Nagoya Univ., <sup>3</sup>RISH, Kyoto Univ.

The earth's radio emission from the auroral region with kilometric wave length (auroral kilometric radiation (AKR)) is known to be transient emissions generated by rapidly accelerated electrons together with sudden auroral activation in the polar magnetosphere. In contrast, the characteristics and relationship with the auroral acceleration of rather continuous AKR emissions are not well understood. We examine the emission using long-term data and report that the continuous AKR emission frequency changes with universal time (UT) as Earth rotates, indicating that Earth is a spin-modulated variable radio source. The observed UT variation of AKR frequency means that the acceleration altitude changes periodically with planetary rotation. The observations indicate that the diurnal wobble of the tilted geomagnetic field in the solar wind flow alters the magnetosphere-ionosphere (M-I) coupling state in the polar magnetosphere, giving rise to periodic variation of auroral particle acceleration altitude. These observations of planetary radio wave properties provide insight into magnetosphere-ionosphere coupling process of the planetary magnetosphere.

Keywords: planetary radio wave, auroral kilometric radiation, spin modulation, variable radio source

## Key parameter of planetary magnetospheric configuration and dynamics

Keiichiro Fukazawa<sup>1\*</sup>

<sup>1</sup>Research Institute for Information Technology, Kyushu University

It has long been recognized that the rapidly rotating magnetospheres of Jupiter and Saturn differ greatly from that of the Earth where rotational effects are largely confined to the plasmasphere. In addition to rapid rotation Jupiter and Saturn both have sources of plasma within the magnetosphere: the volcanos on Io and the ice geysers on Enceladus while the main sources of plasma at the Earth are the solar wind and ionosphere. The magnetic moments of the two rotating gas giants are much larger than that at Earth although the surface field at Saturn is about the same as the Earth's because of its larger radius. At the Earth magnetospheric dynamics are largely controlled by the interplanetary magnetic field and reconnection while at Jupiter and Saturn the solar wind dynamic pressure is more important. Internal processes are also more important at Jupiter and Saturn than at the Earth.

We have performed the MHD simulation of Earth, Jupiter and Saturn then found the each magnetosphere has a unique character. In particular, we have obtained the vortex configuration in magnetospheric convection from Saturn's results and it seems that the formation of vortex may be related to the cushion region where is the space between plasma corotation region and magnetopause. From the simple calculation, the cushion region is controlled by the planetary rotation speed and intrinsic magnetic field. Thus in this study we perform the MHD simulation of magnetosphere with changing the speed of rotation and magnitude of magnetic field to see how the magnetospheric configuration varies. In addition, we discuss the simulation results compared to the previous results of Jovian and Kronian magnetosphere.



## Study of occurrence processes of the Jovian substorm-like events: Examination of an internal drive hypothesis

Takahiro Mizuguchi<sup>1\*</sup>, Hiroaki Misawa<sup>1</sup>, Fuminori Tsuchiya<sup>1</sup>, Takahiro Obara<sup>1</sup>, Satoshi Kasahara<sup>2</sup>

<sup>1</sup>PPARC, Tohoku University, <sup>2</sup>ISAS/JAXA

The observations of the Galileo revealed that there were quasi-periodic flow bursts of energetic particles and the characteristic variation of the north-south component of magnetic field implying magnetic reconnections in the Jovian magnetosphere. Galileo also observed quasi-periodic variation of spectral indexes of energetic ions (slope of the energy spectra in a log-log plot). These imply periodic thinning and thickening of the plasma sheet with a repetition period of 2.5 - 4 days. The signatures of these events were similar to the terrestrial substorm, so they are called "substorm-like events".

In the preceding studies (Kronberg et al., 2007; Woch et al., 1998), their generation processes are proposed as follows based on a hypothesis of plasma mass-loading in the Jovian magnetotail region. First, the magnetotail is stretched because of the large centrifugal force by the rapid rotation and heavy ions. Second, a reconnection occurs and a plasmoid is released. Third, the magnetic field configuration returns to the initial (non-stretched) state, at the sometime the magnetotail stretching starts again and the cycle repeats to make the periodicity.

In this study, we have examined the plasma mass-loading hypothesis by investigating the plasma density inside the plasma sheet by using the data obtained by the Plasma Wave Subsystems (PWS), Energetic Particle Detector (EPD) and Magnetometer(MAG) on-board the Galileo.

At first, we estimated the local electron density by using the plasma frequency. To estimate the occurrence frequency of the substorm-like events, we used two methods; One is to use north-south component of the magnetic field as devised by Vogt et al. (2010) (MAG event). The other is to use narrowband KilOMetric radiation (nKOM) as a signature of the occurrence of the event (nKOM event) to make up the expected azimuthal occurrence restriction of the MAG event. We identified 172 MAG events and 69 nKOM events from the 9 Galileo orbits for 1996-1999. As a result, there was a positive correlation between the local electron density and the occurrence frequency of the events. This result strongly suggests that the substorm-like events tend to occur when the plasma loaded to the Jovian magnetotail region is large.

Second, we estimated the plasma mass-loading rate by using the calculation method proposed by Kronberg et al. (2007). We selected two events for the G2 and the G8 orbits. In order to estimate the mass-loading rate, we also estimated the half-thickness of the current sheet. As a result, the mass-loading rate for the G2 orbit was larger than that of G8. On the other hand, the occurrence frequency and the electron density in the G2 orbit were also larger than those of the G8. This result suggests that the large plasma mass-loading rate causes increase of the plasma loaded to the Jovian magnetotail region, and also increase of the occurrence frequency of the substorm-like event.

We discussed the long-term correlation between the variations of the occurrence frequency of the event and the Io torus activity. It is confirmed that there was a positive correlation between the intensity variations of [SII] optical emission of Io torus derived by Nozawa et al.(2005) and the occurrence frequency variations of the events for 1997-1999. This result implies that the occurrence of the event is controlled by variations of Io torus. On the other hand, there was no or very weak correlation between the high solar wind dynamic pressure state and the occurrence frequency of the events. And there were not any clear peaks near the characteristic repetition period of the events on the Fourier spectrum of the solar wind pressure. These results indicate the periodic occurrence of the substorm-like event cannot be explained only by the variations of the solar wind pressure.

We conclude that the plasma mass-loading hypothesis could explain the driving mechanism of the substorm-like event.

**Keywords:** Jupiter, Jovian magnetosphere, magnetospheric dynamics, substorm, plasma density, Galileo

## Jupiter's decametric Io-C modulation lanes observed by LWA1

Kazumasa Imai<sup>1\*</sup>, Tracy Clarke<sup>2</sup>, Koichi Fukushima<sup>1</sup>, Akiya Ujihara<sup>1</sup>, Masafumi Imai<sup>3</sup>

<sup>1</sup>Kochi National College of Technology, <sup>2</sup>Naval Research Laboratory, <sup>3</sup>Department of Geophysics, Graduate School of Science, Kyoto University

Frequency-time dynamic spectra of Jupiter's decametric emissions display a complex structure on several different time scales. One of the characteristic spectral patterns on a few seconds time scale is the modulation lanes, which were discovered by Riihimaa in 1968. We have developed a model for the mechanism responsible for their production in which the free parameters have been adjusted to provide a very close fit with the observations [Imai et al., 1992;1997;2002].

In our model, we propose the existence of a grid-like interference screen composed of field-aligned columns of enhanced or depleted plasma density located along the longitudinal direction near satellite Io's orbit. We assume that the radio emitting frequency is very close to the cyclotron frequency at the source, and the shape of the radio beam structure is a thin-walled hollow-cone which has a fixed opening cone half-angle. The line of radio source consisting of the points along the axis of the Io-activated flux tube is also assumed to be located downstream, shifted eastward in the longitudinal direction from the instantaneous Io flux tube, for the case of Io related emissions. As a band of frequency components emitted from near the foot of an excited tube of magnetic flux passes through the screen, interference patterns of slightly different orientations are produced by the radio emissions at the different frequencies. The corotation of this set of interference patterns with Jupiter results in the sloping modulation lanes of the observed dynamic spectrum.

The Long Wavelength Array (LWA) is a low-frequency radio telescope designed to produce high-sensitivity, high-resolution images in the frequency range of 10-88 MHz. The Long Wavelength Array Station 1 (LWA1) is the first LWA station completed in April 2011, and is located near the VLA site in New Mexico, USA. LWA1 consists of a 256 element array, operating as a single-station telescope. The first Jupiter radio observation using LWA1 was made by Tracy Clarke (PI) from December, 2011. The observed Io-C dynamic spectrum on March 10, 2012 shows the modulation lanes of both left and right hand polarization components share the same lane structure. It indicates that the both left and right hand Io-C radiations are emitted from the southern hemisphere. And the locations of the radio sources along the Jupiter's magnetic field should be very close. This is very important information to understand the Jupiter's radio emission mechanism.

### References

- [1] K.Imai, L.Wang, and T.D.Carr, A Model for the Production of Jupiter's Decametric Modulation Lanes, *Geophysical Research Letters*, Vol.19, No.9, pp.953-956, 1992.
- [2] K.Imai, L.Wang, and T.D.Carr, Modeling Jupiter's Decametric Modulation Lanes, *Journal of Geophysical Research*, Vol.102, No.A4, pp.7127-7136, 1997.
- [3] K.Imai, J.J.Riihimaa, F.Reyes, and T.D.Carr, Measurement of Jupiter's Decametric Radio Source Parameters by the Modulation Lane Method, *Journal of Geophysical Research*, Vol.107, No.A6, 10. 1029/2001JA007555, 2002.

**Keywords:** Jupiter radio, decametric wave, modulation lane, radio source, radio emission mechanism, LWA

## Objective detection of weak Jovian decametric radiation by using a short baseline interferometer system

Tomoyuki Nakajo<sup>1\*</sup>, Takashi Aoyama<sup>1</sup>, Hiroshi Oya<sup>2</sup>

<sup>1</sup>Fukui University of Technology, <sup>2</sup>Tohoku University

### 1.Introduction

Jovian decametric radiation (DAM) is a well-known radio wave radiated from auroral region at Jupiter. Observation of DAM is very important for study of planetary magnetosphere different from Earth. Especially, occurrence probability of DAM is important for monitoring the activity of Jovian magnetosphere.

However, standard detection techniques of DAM can be affected by subjective view of observer because the judgment is based on the morphology observed in the received signals. In this study, we performed data analysis for a short baseline interferometer system in order to establish a more objective detection technique for DAM.

### 2.A short baseline interferometer system in Fukui University of Technology (FUT)

The interferometer system consists of 3 baselines with 100 m class baseline length. The observation is usually carried out with the observing frequency of 23.31 MHz. In the system, fringe waveforms are digitized by 5 Hz sampling frequency and stored in HDD.

### 3.Fringe correlation technique

In order to detect the fringe wave of Jupiter origin, we calculated normalized correlation coefficient between observed and theoretical fringe waveforms. The theoretical fringe waveform is calculated under assumption that DAM is radiated continuously with a constant intensity. We judge the detected signal to be DAM in the case the correlation coefficient exceeds a given threshold value. In the analysis, we set the threshold value as 4 sigma in probability distribution of obtained correlation coefficients. We were forced to select the integration time as about 2 hours which is too long compared to typical duration of DAM because of the short baseline length in our interferometer system. Therefore, it should be noted that a short duration DAM may not be detected in the present study.

### 4.Validity of fringe correlation technique

We evaluated the validity of fringe correlation technique based on the following 3 viewpoints.

#### (1)Comparison with standard CML-Io phase diagram

We calculated a CML-Io phase diagram by using only the observation result in the present study and compared with the standard diagram. The result shows the diagram obtained in the present study is similar to the standard one, which indicates the validity of fringe correlation technique.

#### (2)Comparison with the dates expected a shock structure of solar wind reaches Jupiter

Next, we compared the detection dates of DAM with the dates expected a shock structure of solar wind reaches Jupiter. The dates expected a shock structure of solar wind reaches Jupiter were calculated by using the solar wind data of WIND spacecraft. The analyses were performed by using the data obtained within one month before and after the opposition. As the results, it was confirmed that the almost signals detected in non-Io phase were received within one day before and after the date a shock structure of solar wind reaches Jupiter.

#### (3)Comparison with the observation in Nancay observatory

Finally, we compared with the wideband spectrum data in Nancay observatory. The result in 2009 and 2010 shows the dates DAM were detected in FUT and Nancay are mostly agreement, which indicates the validity of detection technique in the present study. On the other hand, we could not detect distinct DAM signals in Nancay data of 2007 and 2008 although signals were detected in FUT. This result probably shows fringe correlation technique can be more highly sensitive than the spectrum observation in Nancay.

### 5.Discussion and future study

We confirmed that the fringe correlation technique is very effective for objective detection of weak DAM emission. The results indicate a majority of non-Io DAM is radiated within one day before and after a shock structure of solar wind reaches Jupiter. In addition, we might detect a new Io-related component in CML-Io phase diagram. We need to continue the observation and develop a new interferometer network with a few km baseline lengths which can detect a short duration DAM signals.

Keywords: Jupiter, decametric, radio, interferometer, solar wind

## Development of the Telescope Dedicated to the Observations of Planets and Exoplanets at Haleakala, Hawaii: IX

Yasumasa Kasaba<sup>1\*</sup>, Takeshi Sakanoi<sup>1</sup>, Masato Kagitani<sup>1</sup>, Hiromu Nakagawa<sup>1</sup>, Isabelle Scholl<sup>2</sup>, Jeffrey Kuhn<sup>2</sup>, Shoichi Okano<sup>2</sup>, Takahiro Obara<sup>1</sup>, Yasuhiro Hirahara<sup>3</sup>

<sup>1</sup>Tohoku Univ., <sup>2</sup>Univ. Hawaii, <sup>3</sup>Nagoya Univ.

We have run the project to develop the telescope dedicated to the observations of planets and exoplanets at the summit of Mt. Haleakala of Maui Island, Hawaii, under the international consortium formed with the Institute for Astronomy (IfA) / Univ. of Hawaii (UH) and several groups in USA, Mexico, Canada, and Europe. This telescope project consists of several parts: The main is the new construction of the 1.8m off-axis telescope named 'PLANETS'. We also have two sub telescopes, i.e., the 80cm telescope operated by Univ. Hawaii, and the 60cm telescope operated by Tohoku Univ.

Clear sky and good seeing condition are definitely important for any ground-based observations. The Haleakala High Altitude Observatories at the summit of Mt. Haleakala is not the highest place (elv. 3050m), but one of the best sites with clear skies, good seeing, low humidity conditions. It can easily be operated by its good accessibility from Japan, the airport, the town, associated with a good engineering facility, ATRC (Advanced Technology Research Center) of the IfA/UH.

At there, our group has been operating a 40cm Schmidt-Cassegrain telescope, observing faint atmospheric and plasma features such as Io plasma torus, Mercury, Lunar sodium tail, and so on. Atmospheric escapes from Mars and Venus and the exoplanets close to mother stars are also possible topics as the next extensions.

The 1.8m PLANETS (Polarized Light from Atmospheres of Nearby Extra Terrestrial Planets) telescope will have the first light in 2014, in the earliest case. It has an off-axis primary mirror (provided from Tohoku Univ.) with a diameter of 1.8 m. With the support of state-of-the-art adaptive optics and masking technologies, we can avoid diffraction due to a spider structure that holds a secondary mirror and to minimize the scattered light from mirror surfaces as far as possible. With the instruments set to Gregorian focus on an equatorial mount and Coude focus for large-sized spectrometers, it can provide us a unique facility for spectroscopic and polarimetric observations of faint environments around the bright bodies, like planetary environments, stellar disks, etc. In 2013, we start the polishing for the a ultra-smooth mirror surface, the roughness of less than 1/20 lambda, with a new polish technology called HyDra, a water jet polishing technology developed by a group at Univ. Nac. Aut. de Mexico (UNAM). (This project is also a test for this new technology applied to off-axis mirrors.)

The UH 80 cm with equatorial mount is completely optimized to the polarimetric studies. It is served by Harlinton Center for Innovative Optics (Canada), and operated by IfA/UH with Kiepenheuer Inst. Sonnenphysik (Germany). The Gregolian optics for the PLANETS will be tested at there.

The 60 cm Cassagrain telescope is now at our Iitate Observatory. We started the reformation of its equatorial mount optimized to the Hawaiian latitude, and will move it to Haleakala before the summer of 2013. It is small-sized but unique because it has Coude focus for relatively large-sized instruments. It will not only be used for the infrared / spectroscopic observation which cannot be done by the current 40cm, but also the instrument testing for the PLANETS.

In the end of 2013, ISAS Exceed EUV space telescope will run on the orbit. In early 2014, joint observation with HST for Jovian activities will be executed. This 60cm telescope will supply the simultaneous and continuous imaging and spectroscopic data for Jovian infrared auroras.

We also continuously run the 40cm Schmidt telescope will also serve the Io torus imaging spectroscopic information.

For promoting the project, M. Kagitani has been staying in Maui and contributing to the optical fiber Echelle spectrograph development. From June 2012, S. Okano officially belonged to ATRC. The instruments developed in our group, i.e., NIR/MIR Echelle spectrograph and MIR heterodyne spectrograph will also contribute to these telescopes.

Keywords: infrared, optical, Haleakala Observatory, Telescope, Planet

## Temperature variation of the cloud top of Venus obtained by photometry observation by LIR onboard Akatsuki

Tetsuya Fukuhara<sup>1\*</sup>, Yuuna Shima<sup>1</sup>, Toru Kouyama<sup>2</sup>, Takeshi Imamura<sup>3</sup>, Masahiko Futaguchi<sup>4</sup>, Makoto Taguchi<sup>4</sup>

<sup>1</sup>Hokkaido University, <sup>2</sup>AIST, <sup>3</sup>ISAS, <sup>4</sup>Rikkyo University

The Japanese Venus Climate Orbiter called Akatsuki was designed to study the meteorology of the Venusian atmosphere, which differs to that of the Earth in composition, density and circulation. Akatsuki was to orbit around Venus in an elongated equatorial orbit with almost the same angular velocity during most of the orbital period as that of the super rotation of the atmosphere at the cloud top altitudes, like a geosynchronous satellite. A 3-D structure of the atmosphere was to be reconstructed by multi-depth imaging using four cameras operating in the mid-infrared to near ultraviolet regions and using the radio occultation technique. The Longwave Infrared Camera (LIR), which mounts an uncooled micro-bolometer array (UMBA), is one of a suite of cameras onboard Akatsuki, designed to take mid-infrared images of Venus with a single band-pass filter of 8.7-12  $\mu\text{m}$ . LIR detects thermal radiation emitted from the layer where the cloud optical depth equals unity. The noise equivalent temperature difference (NETD) of LIR is 0.3 K and absolute temperature can be determined with an accuracy of 3 K. In addition, a cloud tracking technique could retrieve the horizontal wind vector field at the cloud-top height. Unfortunately, Akatsuki failed to enter the orbit because trouble occurred with the propulsion system on December 7, 2010. At present the spacecraft is orbiting the Sun, and it will have a chance to encounter Venus in 2015. During the spacecraft cruising, LIR successfully acquired 52 photometry data of day-side Venus between February and March 2011 at a distance of 1.2-1.7 $\times 10^7$  km. The spatial resolution of LIR and an apparent diameter of Venus being almost equivalent, Venus' disk in the image extends to several pixels that include both Venus and the background radiation. All brightness pixels that included Venus were summarized and the background radiation component were removed from them to estimate a Venus' brightness component. Furthermore, it has been converted to the brightness temperature by using calibration data acquired in the laboratory before the launch and brightness temperature variation of the disk have been obtained. However, the discrete data set has large data gaps. Then, the Lomb-Scargle periodogram, which is better suitable than Fast Fourier Transform, has been applied and been obtained a spectrum. The result shows spectrum peaks at 5-day and 8-day period. The 5-day period may be caused by the super rotation, and the 8-day period may be a planetary-scale wave that has the phase velocity of  $\sim 50$  m/s.

Keywords: Venus, atmosphere, Akatsuki, LIR



## Study of the Venus cloud upper haze

Seiko Takagi<sup>1\*</sup>, Arnaud Mahieux<sup>2</sup>, Valerie Wilquet<sup>2</sup>, AnnCarine Vandaele<sup>2</sup>, Naomoto, Iwagami<sup>1</sup>

<sup>1</sup>Graduate School of Science, the Univ. of Tokyo, <sup>2</sup>Belgian Institute for Space Aeronomy

Venus is covered by H<sub>2</sub>SO<sub>4</sub> clouds floating at 45-90 km. Despite Venus cloud is identified by previous Venus observation, there are many unknown things about Venus cloud because of small number of Venus observations. Moreover, knowledge of Venus cloud upper haze layer(70-90 km) is less than upper, middle and lower cloud remarkably because most of Venus probes observed only below the upper cloud layer (under 70km).

Solar Occultation at Infrared(SOIR), which is a part of the spectroscopy on board Venus Express, is designed to measure at high resolution the atmospheric transmission in the IR (2.2-4.3  $\mu$ m) using solar occultations. SOIR observe Venus atmosphere and cloud existed at high altitude (60-220 km), any latitude and longitude. In this study, analysis of SOIR data obtained between 2006 and 2009 is performed to obtain knowledge of Venus cloud upper haze layer.

Altitude distribution and time variation of upper haze extinction and mixing ratio are derived from SOIR data. Mixing ratio vertical distribution shows that haze creation is more dominant than vertical eddy diffusion at above 90 km. It is speculated that sulfide is contained in haze from comparison of this study and mixing ratio vertical distribution of SO/SO<sub>2</sub>. Mixing ratio vertical distribution shows that vertical eddy diffusion is more dominant than haze creation at 70-90 km. It is speculated that sulfide is contained in haze from comparison of this study and time variation and latitude distribution of SO/SO<sub>2</sub>.

Keywords: Venus, cloud, Venus Express, SOIR

## Venusian upper hazes observed by Imaging-Polarimetry system HOPS

Takayuki Enomoto<sup>1\*</sup>, Takehiko Satoh<sup>2</sup>, NAKATANI, Yoshikazu<sup>3</sup>, Takashi Nakakushi<sup>4</sup>, Takao M. Sato<sup>5</sup>, Shoko Ohtsuki<sup>6</sup>, Mayu Hosouchi<sup>7</sup>

<sup>1</sup>Grad.Univ.Advanced Studies, <sup>2</sup>Japan Aerospace Exploration Agency, <sup>3</sup>Kyoto University, <sup>4</sup>Wakayama University, <sup>5</sup>NICT, <sup>6</sup>Senshu University, <sup>7</sup>University of Tokyo

Physical properties of the aerosols in the Venusian upper atmosphere can be derived by measuring the polarization of light scattered by them. Kawabata et al. [1980] obtained polarization maps of Venus from the data of Orbiter Cloud Photopolarimeter (OCP) onboard the Pioneer Venus Orbiter, and found that numerous haze particles distributed mainly on polar region. Kawabata [1987] and C. J. Braak et al. [2002] analyzed years of data observations and reported that optical depth of the hazes had rapidly declined. The variability of hazes and clouds can change longitudinal balance of solar absorption and atmospheric dynamics.

Two dimensional polarization maps are in general advantageous as they allow us to selectively pick up the local characteristics. We developed a planetary imaging-polarimetry system HOPS (Hida Optical Polarimetry System), which can take polarization maps as OCP, and do observations for the purpose of monitoring of Venusian upper hazes.

The optical system of HOPS is composed of combination of a Wollaston prism and a half wave retarder, and the observation channels are 930, 647(650), 548(546), 438nm. One observation includes a total of four shots with the retarder position angle is incremented by 22.5 degrees. By arithmetic operations of the data, the degrees of linear polarization are obtained accurately after removing the effects of 'unevenness of the CCD sensitivities' and 'transparency of the atmosphere'. However, the uncertainties of registration and resulting polarization errors caused by the effect of the time-variable atmospheric turbulence are problems for planetary observations, which need to be taken care of.

The observations were performed in Hida observatory of Kyoto Univ. on May, Aug., and Oct. 2012. The phase angles of Venus at that time were 128, 85 and 58 deg., and apparent diameters are 42, 21, 14 arc second, respectively. The scale of one CCD pixel on the 65cm refractor is about 0.3 arc second, so the diameter of images of Venus on Aug., whose apparent diameter was about 21 arc second, was about 70pix. Polarization maps of this resolution are enough to pick up the local characteristics as PVO.

As a quick-look of the observations, we compared the data of 548nm and 930nm, whose channels are close to those of Kawabata et al. [1980], with them. The disk-integrated polarization degrees of 548nm matched with the past data. In contrast, the 930nm data were -3% ~ -2% while those of PVO were -2 ~ -1%. By comparison of equatorial and polar region, it was found that polarization degree of polar region is more negative than PVO data, this relatively lowered the disk-integrated polarization degree. These values are, however, less negative than those of ground-based observations in 1960s, this may indicate that the distribution of haze particles at the time of HOPS observation is somewhat similar to the situation of PVO arrival at Venus.

We are planning to observe at other phase angles and developing the calculation code of radiative transfer including polarization for the purpose of quantitative evaluations.

Keywords: Venus, Haze, Imaging-Polarimetry, Ground-based observation



## Latitudinal cloud structure in the Venusian northern hemisphere evaluated from VEX/VIRTIS with GCM

Morihiro Kuroda<sup>1</sup>, Takeshi Kuroda<sup>1</sup>, Yasumasa Kasaba<sup>1\*</sup>, P. Drossart<sup>2</sup>, G. Piccioni<sup>3</sup>, Kohei Ikeda<sup>4</sup>, Masaaki Takahashi<sup>5</sup>

<sup>1</sup>Tohoku Univ., <sup>2</sup>Observatoire de Paris, <sup>3</sup>INAF-IAPS, <sup>4</sup>JAMSTEC, <sup>5</sup>Univ. Tokyo

The latitudinal characteristics of Venusian northern cloud, i.e., opacity, top temperature and top altitude are evaluated from the Venus Express/VIRTIS observations. The cloud optical thickness in the polar region (~65 degN) is ~1.5 times larger than in middle latitudes. It suggested that in the polar region the amount of cloud particles is larger or the properties of cloud particles are different. The averaged cloud top temperature is uniform in 0 - 40 degN (232±2 K), gradually decreases north to 70degNN (223±5 K), and increases again to north pole (233±6 K). On the other hand, the averaged cloud top altitude is monotonously decreasing from equator (68.2±1.6 km) to north pole (58.3±1.0 km). Since the cloud top altitude sharply decreases beyond the polar region (~65 degN), the structure of Venusian polar vortex is affected by the decreasing of cloud top. The abundance of carbon monoxide under the cloud layer was measured using Band Ratio Technique constructed by Tsang et al. (2009). As a result, the mixing ratio increases from 16±3 ppm at equator regions to 24±5ppm at 70 degN, and it decreases to 19±5 ppm at 80 degN. Furthermore, there is a negative correlation between the CO abundance and cloud top temperature, and the peak of CO abundance is located in the cold collar regions (~70 degN). Since CO under the cloud is transported from the upper layer, the CO enhancement in the cold collar can be interpreted the down-welling region of planetary-scale circulations, i.e., the Hadley-Circulation. We tried to evaluate the suggestion with a Venusian General Circulation Model (GCM). As a result, the cloud top altitude is monotonously decreasing from equator (67.3 km) to north pole (59.3 km) and the cloud top temperature is almost same from equator to 40o N (234 K), and gradually decreasing to 70 degN (228 K), and increasing toward north pole (242 K) again. In addition, the mean meridional stream-function indicates the existence of down-welling of Hadley-Circulation at the cloud top regions around 70 degN. It can be interpreted that the Venusian polar vortex structures (polar dipole and cold collar) seen from infrared wavelength are created from decreasing of cloud top due to the Hadley-Circulation.

Keywords: Venus, Cloud, altitude, latitude, Venus Express, GCM

## Development of a sulfuric acid cloud transfer/condensation/evaporation scheme in a Venusian GCM

Kato Fumiya<sup>1\*</sup>, NITTA, Akira<sup>2</sup>, KURODA, Takeshi<sup>1</sup>, KURODA, Morihiro<sup>1</sup>, KASABA, Yasumasa<sup>1</sup>, TAKAHASHI, Masaaki<sup>2</sup>

<sup>1</sup>Tohoku University, <sup>2</sup>University of Tokyo

We are investigating the cloud formation, chemical reactions, and their radiative effect which affect the atmospheric dynamics in the Venusian middle atmosphere, using a VGCM (Venus General Circulation Model). Recently we introduced evaporation/condensation processes of the sulfuric aerosol into the VGCM developed by Ikeda [2011], and reproduced the latitudinal/vertical distribution of the sulfuric aerosol which is consistent with previous observations. In this presentation, we will show the results and the future steps of our research.

Venusian sulfuric acid cloud deck, which exists in the altitude of 50km-70km, is considered to have a strong influence on the thermal balance of the Venusian atmosphere. The component of the cloud particle is mainly sulfuric aerosol which is formed by the reactions between SO<sub>2</sub>, O and H<sub>2</sub>O. The sulfuric acid droplets are divided into 4 groups according to the size; mode1 (0.3μm), mode2 (1.0μm), mode2' (1.4μm) and mode3 (3.56μm) as defined in Crisp. [1986]. Each mode has its own characteristics of vertical distribution and thermal absorption efficiency, so reproducing the vertical/latitudinal distribution of those modes in the numerical model is important to simulate the general circulations in the Venusian atmosphere.

We have investigated the cloud distributions in the Venusian atmosphere using a VGCM based on the CCSR/NIES/FRCGC AGCM [Ikeda, 2011]. The model has 32(latitude) X 64(longitude) grid points and 52 vertical levels from the surface up to 95km. It successfully reproduces the zonal and meridional winds including super-rotation and Hadley circulation in the Venusian atmosphere. The current model calculates the radiative effects of clouds and molecules from fixed distributions defined in Crisp [1986] and Pollack et al. [1993], so we plan to implement into the model the radiative effects which will be consistent with the calculated cloud distributions, as well as the chemical reactions for production of the clouds.

We introduced the evaporation/concentration process of H<sub>2</sub>SO<sub>4</sub> and simulated the evaporation of aerosols in the lower atmosphere which has the higher temperature and the condensation of aerosols in the upper atmosphere. The model calculates the saturated mixing ratio in each grid from the saturated vapor pressure curve derived from Ayers [1980], and compared it to the H<sub>2</sub>SO<sub>4</sub> mixing ratio at the grid. We assumed that if the H<sub>2</sub>SO<sub>4</sub> mixing ratio (sum of vapor and cloud) is larger than the calculated saturated mixing ratio, the supersaturated H<sub>2</sub>SO<sub>4</sub> concentrates as an aerosol, and if not the H<sub>2</sub>SO<sub>4</sub> aerosol all evaporates. The generated H<sub>2</sub>SO<sub>4</sub> aerosols are distributed into 4 modes at each altitude according to the abundance ratio based on the observation [Crisp, 1986]. We are implementing the effects of latent heat by the condensation /evaporation using the method of successive approximation.

Because of this improvement, every mode of the cloud now evaporates below 50km altitude. After the calculation of 1 Venusian day (117 terrestrial days), mode 3 aerosol gets the equilibrium state at 50km altitude.

Also the amount of mode2 aerosol largely decreased in low and mid latitudes of 60km-80km altitude, while increased in the atmosphere above 80km in all latitudes and 60km-80km altitude in high latitudes, in comparison with the model without the evaporation/concentration processes [Kuroda et al., 2013]. We consider that the difference is because the sulfuric aerosol is enhanced to evaporate especially in the equatorial middle atmosphere where the temperature is high, and the transport of H<sub>2</sub>SO<sub>4</sub> to higher altitudes and latitudes by Hadley circulation is enhanced due to the phase change.

We will continue to improve our model to increase the accuracy of the simulation of the vertical/latitudinal cloud distribution. In the presentation, we plan to show the numerical results with radiative effects and chemical reactions which is connected to the cloud formation.

Keywords: Venus, GCM, sulfuric cloud, atmospheric material transport

## Temperature distributions in the Venus O<sub>2</sub> night airglow layer by ground-based observations

Shoko Ohtsuki<sup>1\*</sup>, Naomoto Iwagami<sup>2</sup>, Severine Robert<sup>3</sup>

<sup>1</sup>Senshu University, <sup>2</sup>University of Tokyo, <sup>3</sup>Belgian Institute for Space Aeronomy

Venus 1.27-micron O<sub>2</sub> night airglow can be used as a probe of chemistry and dynamics at around 95 km. The enhanced rotational temperature at around the anti-solar point found from the O<sub>2</sub> airglow has been supposed to indicate the evidence of downflow. However, the nightside temperatures at 90-100 km found by SPICAV/VEX differ from those by the airglow.

We conducted 5-days monitoring observation of the airglow to detect the planetary-scale waves with CSHELL/IRTF from 11-15 July 2012. The 1.27-micron O<sub>2</sub> night airglow in the Venus atmosphere can pass through the Earth's atmosphere with a help of the Doppler shift. We obtained spectral image cubes at the wavelength of R-branch of the airglow band, which includes several rotational lines. In order to cover spectral information continuously, a slit drifted across Venus' nightside disk. The spatial resolution of the image is governed by seeing. The typical seeing was 0.6'' to 1.5'' in our observing run and corresponds to 200-450km at the center of Venus' disk. Under such conduction, we may detect airglow structures of small scales due to atmospheric waves; this is smaller than the region of enhanced airglow having a horizontal scale of ~3000km. We can also derive the hemispherical distribution of the rotational temperature. To coincide with our observations, SOIR/Venus Express stellar occultations were conducted. We can try to compare our horizontal temperature map and vertical temperature profile from SOIR data.

Keywords: Venus atmosphere, airglow, ground-based observation

## The propagation characteristics of short-period gravity waves and acoustic waves in the Martian atmosphere

Ayuka Watanabe<sup>1\*</sup>, Takeshi Imamura<sup>2</sup>

<sup>1</sup>Department of Earth and Planetary Science, Graduate School of Science, The University of Tokyo, <sup>2</sup>Institute of Space and Astronautical Science

There are few observations and theoretical works about short-period waves in planetary atmospheres, because it is difficult to observe them. However, short-period waves suffer less damping by molecular diffusion than long-period waves, so they can propagate to higher altitudes. It is expected that upper atmospheres are affected by the dissipation of such waves.

Here we focus on the Martian atmosphere. In Martian atmosphere, airborne dust absorbs incoming sunlight and heats the atmosphere in short time scales. So short-period gravity waves and acoustic waves might be generated and propagate to high altitudes. Then we studied the propagation characteristics of such waves in the Martian atmosphere by using a non-hydrostatic, linear model which extends from the surface to thermospheric heights.

Keywords: acoustic waves, gravity waves, Martian atmosphere

## Feasibility study of the Mars ionospheric imaging

Atsushi Yamazaki<sup>1\*</sup>, Hiromu Nakagawa<sup>2</sup>, Takeshi Sakanoi<sup>3</sup>, Makoto Taguchi<sup>4</sup>

<sup>1</sup>ISAS, <sup>2</sup>Tohoku Univ., <sup>3</sup>PPARC/Tohoku Univ., <sup>4</sup>Rikkyo Univ.

The planetary atmospheric escape to the outer space is a universal phenomenon for planets, and the escape flux will determine the atmospheric evolution of each planet. Mars of the non-magnetized planet has dry and tenuous atmosphere, and it is a severe environment for the survival of living matter. The observations of the recent Mars Express (MEX) spacecraft have shown that the molecular ion, whose outflow flux is very small conventionally, is escaped in large quantities. In addition, it is pointed out that there is possibility for low energy ions less than a few eV to be escaped. The quantity of escape rate of the atmosphere is one of indispensable values for the study of atmospheric evolution, but it is a physical amount to have the big error. It is caused by the fact that the physical mechanism to cause the escape of the molecular ions and low energy ions is not understood. Many physical mechanisms to the atmosphere escape derived by the solar wind and the solar radiation are suggested, including ionospheric ion outflow, ion pickup, sputtering, Jeans escape, and the outflow caused by the photochemical reaction.

We study possibility of the imaging observation instruments to obtain the two-dimensional structure that has not yet been performed for identification of these scatter mechanism until now. In particular, it is one of aims to catch the two dimensional structure of the ionopause where ionospheric ions escape. A fact that emission intensity of the outflow is very low and the albedo of the main body of Mars is very strong as a stray light, is a reason for the very difficult observation. However, because this observation method is thought as an instrument bringing a breakthrough for study on atmospheric evolution, and because it is predicted that it is an essential technique to future planetary probe, we started the research and development of the basic technology. In this paper an optics design of Mars ionosphere observation equipment is argued for example, and it is hoped that it is a beginning of the universal technique to detect the faint emission around the bright light source.

**Keywords:** Mars ionosphere, Imaging observation, Atmospheric escape, Atmospheric evolution

## Development of multi-fluid MHD simulation code of interaction between the solar wind and unmagnetized planets

Kyohei Koyama<sup>1\*</sup>, Kanako Seki<sup>1</sup>, Naoki Terada<sup>2</sup>, Kaori Terada<sup>2</sup>

<sup>1</sup>Solar-Terrestrial Environment Laboratory, Nagoya University, <sup>2</sup>Graduate School of Science, Tohoku University

Draping of the solar wind magnetic field can form the induced magnetosphere around a planet, even when the planet does not possess any intrinsic magnetic field. It has been pointed out that the solar wind induced escape processes such as the ion acceleration in the draped magnetic field and the ionospheric ion scavenging by penetration of the solar wind magnetic field into the ionosphere play important roles in the atmospheric escape from such an unmagnetized planet. The escape of the planetary atmosphere is an important phenomenon related to evolution of the atmosphere, and numerical simulations are an effective method to understand the global atmospheric escape processes. While there have been many previous studies of the interaction between the solar wind and the upper atmosphere of unmagnetized planets based on hybrid or MHD simulations, these models have not yet succeeded to well reproduce the actual observations, such as a large amount of heavy molecule ion escape observed by Mars Express [Carlsson et al., Icarus, 2006] and difference of velocity between O<sup>+</sup> and H<sup>+</sup> [Lundin and Dubinin, ASR, 1992]. In order to reproduce the dynamics of multi-species plasmas around the unmagnetized planet, multi-fluid MHD approximation, in which each ion species is treated as an individual fluid, is effective. Particularly, it is an advantage of the multi-fluid MHD code that it can include ion-ion collisions and assess their effects on the ionospheric convection numerically. Combining the virtue of existing multi-species [Terada et al., JGR, 2009] and multi-fluid [Najib et al., JGR, 2011] simulations, we have formulated a new multi-fluid code to simulate the solar wind-unmagnetized planet interaction. In this presentation, we report on the formulation and initial results of the multi-fluid MHD simulation code under development.

Keywords: unmagnetized planet, ionosphere, multi-fluid simulation

## Mission data processing and attitude control of the SPRINT-A/EXCEED mission

Fuminori Tsuchiya<sup>1\*</sup>, Atsushi Yamazaki<sup>2</sup>, Takeshi Sakanoi<sup>1</sup>, Kazunori Uemizu<sup>3</sup>, Kazuo Yoshioka<sup>2</sup>, Go Murakami<sup>2</sup>, Yasumasa Kasaba<sup>1</sup>, Masato Kagitani<sup>1</sup>, Ichiro Yoshikawa<sup>4</sup>

<sup>1</sup>Tohoku University, <sup>2</sup>ISAS/JAXA, <sup>3</sup>NAOJ, <sup>4</sup>The University of Tokyo

The mission data processing and attitude control of extreme ultraviolet (EUV) spectroscope (EXCEED) onboard the SPRINT-A satellite are presented. SPRINT-A is an earth-orbiting extreme ultraviolet spectroscopic mission being developed by ISAS/JAXA. Two mission instruments are installed in EXCEED, an EUV spectrograph and a target guide camera, and the final quantification of them has been completed in the beginning of 2013. It is planned to launch on August 2013 and will begin observation of Venus and Jupiter on October. Collaboration with Hubble Space Telescope is approved on January 2014. The target guide camera is designed to capture a part of a target planet disk whose light is reflected from the front side of a slit. Mission data processor (MDP) acquires the image every 3 seconds, calculates the centroid position of the disk on the image, and sends it to the attitude control system. While the pointing accuracy of the bus system is at most 2 arc-minutes, scientific requirement for spatial resolution is 10-arcsec to derive radial structure of Io plasma torus and detect plasma emissions from ionosphere, exosphere and tail separately (Venus and Mars). The attitude control system keeps the centroid position with an accuracy of 10 arc-seconds to achieve the spatial resolution required. This pointing correction algorithm is applied to correct slow changes in the pointing direction which is mainly caused by changing thermal input from the sun and earth to the satellite. Though vibrations from reaction wheels installed in the bus system could cause random pointing error, the amplitude is estimated to be 1 arc-second for SPRINT-A. To test the centroid calculation algorithm, a small pinhole image was taken by the guide camera with flight-model optical layout. The size and brightness of the pinhole were equivalent to those of Jupiter. Changing the pinhole position, acquiring and processing of the image and centroid calculation were repeated many times. The designed algorithm has been confirmed to work well and the stability of the centroid position was found to be less than 0.3 arc-second. Final interface test between EXCEED and attitude control system is planned on March 2013.



## Study of the plasma environment near Ganymede by the Galileo spacecraft observation

Shinya Watanabe<sup>1\*</sup>, Takayuki Ono<sup>1</sup>, Atsushi Kumamoto<sup>1</sup>, Yuto Katoh<sup>1</sup>

<sup>1</sup>Department of Geophysics, Graduate School of Science, Tohoku University

Ganymede is one of Jovian moons and is known as the only satellite that has intrinsic magnetic field. Since Ganymede is located in the Jovian magnetosphere, magnetospheric plasma corotating with Jovian rotation period of 10 hours always blows toward Ganymede at a relative velocity of 176 km/s. So, the characteristic plasma environment is formed around Ganymede due to the interaction between Ganymede's magnetosphere and Jovian magnetospheric plasma.

Although previous studies discussed the morphology of Ganymede's magnetosphere and its plasma environment, most of them are still well unknown and understanding of the interaction is necessary to reveal processes occurring in the Ganymede's magnetosphere.

In the present study, we have analyzed plasma waves observed near Ganymede by the Plasma Wave Subsystem (PWS) and the Magnetometer (MAG) on board the Galileo spacecraft. In particular we have analyzed emissions enhanced at Upper-hybrid resonance (UHR) frequency and have identified its spatial distribution around Ganymede from the data obtained during the four flybys (G01, G02, G07, G29) in which the UHR emissions are clearly seen among the all six Ganymede flybys. Based on the identified UHR frequency and the electron cyclotron frequency estimated from the background magnetic field intensity by MAG, we have analyzed the spatial distribution of electron density around Ganymede. The electron cyclotron frequency is estimated to be 5~20 kHz in the Ganymede magnetosphere. The result of the analysis shows that fUHR is about 20~100 kHz and becomes high when the spacecraft is near Ganymede. The maximum of the electron density is estimated to be 200 cm<sup>-3</sup> when the spacecraft is at the location closest to Ganymede of 264 km altitude during the G02 orbit.

The Ganymede ambient magnetic field can be classified into three types of condition, (1) both ends are on Ganymede, (2) one end is on Jupiter and another end is on Ganymede, and (3) both ends are on Jupiter. We study the electron density profile and plasma wave measured in each region based on both the MAG data and the trajectory of the Galileo spacecraft. We also analyze the 10 kHz waveform data in order to discuss fine structures of the spatial plasma distribution and plasma waves around Ganymede. By comparing these results to the plasma environment around planets interacting with solar wind and satellites in the planetary magnetosphere, we discuss the characteristic of the Ganymede's magnetosphere.

Keywords: Ganymede, Jupiter, plasma waves, magnetosphere

## Short-term variation of Jupiter's synchrotron radiation: Their relation with the magnetospheric events

Hiroaki Misawa<sup>1\*</sup>, Takahiro Mizuguchi<sup>1</sup>

<sup>1</sup>Planetary Plasma and Atmospheric Research Center, Tohoku University

It is known that Jupiter's synchrotron radiation (JSR) has information on dynamics of the deep inner magnetosphere. Our Tohoku University group has implied that Jupiter's synchrotron radiation in several tens MHz sometimes shows rapid flux variations (RFV) by more than several tens % within a few to several days. It is quite difficult to explain its physical process by present theories on particle transport, such as radial diffusion because of their too fast change. This phenomena recalls the fast particle acceleration and transport in the earth's magnetosphere during substorm events. It is already confirmed that there are substorm like events also in Jupiter's magnetosphere, however, and it has not been revealed whether the events affect the deep inner region.

In order to reveal unknown dynamics of the RFV events in JSR, we have tried to investigate relationship between the RFV events and electromagnetic phenomena in Jupiter's magnetosphere. We have surveyed plasma and magnetic field data observed by Galileo. For searching the RFV events, we have used the daily JSR monitoring data at 327MHz observed using the large radio telescopes of STE Lab, Nagoya University. In this presentation, we show some results of characteristics of the RFV events and make preliminary discussion on their origin.

Keywords: Jupiter, synchrotron radiation, short-term variation, radiation belt, substorm

## Occurrence characteristics of Jovian auroral emissions in the low-latitude region

Kazuyuki Yamamoto<sup>1</sup>, Hiroaki Misawa<sup>1\*</sup>, Fuminori Tsuchiya<sup>1</sup>, Takahiro Obara<sup>1</sup>

<sup>1</sup>Planet. Plasma Atmos. Res. Cent., Tohoku Univ.

Jupiter has large magnetosphere and bright auroral emissions in the polar region. In the low latitude region, defined between the main oval region and the Io footpath latitudinal region, "patchy emission" and/or "extended emission" sometimes appear at the postnoon sector as an extended emission from the main oval region to near the Io footpath latitudes. Although these emissions reflect some activities of the Jovian inner to middle magnetosphere, it is little known what magnetospheric activities contribute to the auroral emission. In this study, we have researched their variations and occurrence characteristics to understand physical processes of the inner to middle magnetospheric activities using the data of Jovian UV and IR auroras observed with Hubble Space Telescope (HST) and NASA InfraRed Telescope Facility (IRTF). From the HST campaign observations in 2007, it is suggested that the low-latitude emissions have the duration time of several tens of hours and shift their emission regions in the direction of positive system 3 longitude; i.e., the emission region lagged from the corotation. The shift velocities were derived to be several percent to more than ten percent. The velocities cannot be explained only by magnetic drift of electrons with the energy of several tens keV which is typical for UV aurora. The past in-situ plasma observations by Voyager and Galileo showed that the plasma bulk velocity in the inner to middle magnetosphere is a few to ten-odd percent slower than corotation speed. These values are similar to the lag of the extended auroral emissions. Thus, it is plausible that the lag of the low-latitude emissions is mainly caused by the corotation lag of the plasma in the Jovian magnetosphere.

In order to investigate causality of occurrence of the low latitude auroras, we have surveyed the IR aurora data for the Galileo's Jupiter observation period. Mauk et al. [Nature, 2002] indicates one event of low-latitude patchy emission corresponding injection. In this study, we have examined correspondence between low-latitude emission and the phenomena relating to injection; i.e., injection, the location of Galileo satellites, solar wind and nKOM. We identified four low-latitude emission events for totally 43 days of the observation by IRTF for 1996 - 2000. As the result, we could not confirm the correspondence between the low-latitude emission and injection due to lack of the Galileo data. Furthermore, we could not find relationship between the low-latitude emission and injection relating phenomena. The duration time of low-latitude emission identified in this study was a few dozen hours, while it is reported that the duration time of injection is at most 12 hours. This implies that the low-latitude emissions identified in this study are a new type and different from the event identified by Mauk et al. (2002). The confirmation of types of the low-latitude auroras and investigation of their occurrence processes are deferred in the future studies.

Acknowledgement: We would greatly appreciate to Prof. J. T. Clarke, Boston University, for providing the data of HST ACS/SBC and Prof. T. Satoh, JAXA/ISAS, for providing the data of NASA/IRTF.

Keywords: Jupiter, Jovian magnetosphere, aurora, injection

## Statistical analysis of the repetition frequency of S-bursts of Jovian decametric radiation

Suguru Kakimoto<sup>1</sup>, Atsushi Kumamoto<sup>1\*</sup>, Takayuki Ono<sup>1</sup>, Yuto Katoh<sup>1</sup>, Hiroaki Misawa<sup>1</sup>

<sup>1</sup>Tohoku University

Repetition frequency of S-bursts of Jovian decametric radiation has been statistically analyzed based on the datasets of ground-based observations performed at the observatories of Tohoku University since 1985. In the Jovian magnetosphere, the radio waves are generated in decametric wavelength range due to the interactions between the rotating magnetic field and the satellite Io. Among them, the S-bursts are intense emissions which show quasi-periodic frequency drift on a time scale of msec. The typical repetition frequencies are within 2-400 Hz [Carr and Reyes, 1999]. Based on the studies of the Earth's ionospheric Alfvén resonator (IAR), Ergun et al. [2006] proposed that the periodicity of the S-bursts was caused by the Jovian IAR. According to the hypothesis, it is expected that the repetition frequency of S-bursts and IAR increase as the solar zenith angle at the Io footprint increases and plasma density in the Jovian ionosphere decreases. In order to verify the Jovian IAR hypothesis, we have analyzed repetition frequency of S-bursts.

We have analyzed datasets obtained by ground-based observations performed at the observatories of Tohoku University since 1985. The datasets obtained by new HF receiver system installed at Yoneyama observatory (141.2E, 38.6N) in 2012 are also utilized in the analyses. The frequency range, frequency and time resolutions of the new HF receiver system were 21.5 - 37 MHz, 1.2 kHz, and 0.8 msec, respectively. As a result of the statistical analysis of the datasets since 1985, it was found that the repetition frequency of S-bursts decreases as the increase of solar zenith angle at the Io footprint on the Jovian ionosphere. The result was opposite to the expectation. Some previous studies reported that the activity of the Earth's aurora depends on the solar zenith angle in the ionosphere [Newell et al., 1997]. They explained that it was because the growth of the feedback instability in IAR depended on the conductivity of the ionosphere. If the auroral electron precipitations increase in Jovian IAR when the solar zenith angle increase just as in the Earth's IAR, we can expect that the repetition frequency of S-burst decreases due to the increase of the plasma density and the temperature in the ionosphere.

**Keywords:** Jovian decametric radiation, S-bursts, Ionospheric Alfvén resonator, Solar zenith angle dependence, Jovian ionosphere, Feedback instability

## Time variability of [OI] 630nm emission from Enceladus torus

Kunihiro Kodama<sup>1\*</sup>, Masato Kagitani<sup>1</sup>, Shoichi Okano<sup>2</sup>

<sup>1</sup>Geophys. Sci., Tohoku Univ., <sup>2</sup>IfA

There are many icy atoms and moleculars in Saturn's inner magnetosphere. This materials distribute like a torus, so called enceladus torus.

We successfully detected the forbidden line emission of atomic oxygen [OI] 630 nm at Enceladus torus by ground-based observation carried out in May, 2011~.

We had assumed that main process for this emission is electron impact excitation. But other process like as photo dissociation of molecules as H<sub>2</sub>O and OH are not ignorable. So we continued the observation to understand featur of [OI] 630 nm emission on the torus. Long term observation will show many hint about relation between the emission and environment. However, lack of high-quality data restricted the data point against time.

Now we improved the analysis method and it enabled us to use mid-high quality data. The additional usable data was used for derivation of emission.

In this presentation, I will report results of new analysis.

Keywords: Enceladus, saturn, groundbased